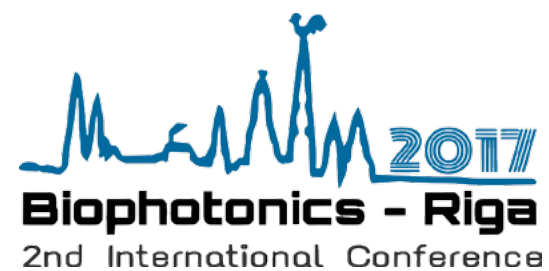


PROGRAMME & ABSTRACTS

Riga, Latvia | 27 – 29 August | 2017



27 - 29 August, 2017

PROGRAMME & ABSTRACTS

Riga, Latvia

Supported by

- National Research Programme "Cyber-physical systems, ontologies and biophotonics for safe&smart city and society", Project "BIOPHOTONICS: Imaging, Diagnostics and Monitoring" under grant agreement #10-4/VPP-4/11
- UL – University of Latvia
- ASI – Institute of Atomic Physics and Spectroscopy
- SPIE – International Society for Optics and Photonics
- SLOB – Starptautiskā Lietišķās Optikas biedrība (The International Society for Applied Optics)

Conference organizers

Scientific Committee

Prof. Stefan Andersson-Engels, Ireland
 Prof. Ekaterina Borisova, Bulgaria
 Prof. Ricardas Rotomskis, Lithuania
 Prof. Janis Spigulis, Latvia
 Prof. Valery Tuchin, Russia

Local Organising Committee

Prof. Janis Spigulis (Chair)
 Dr. Ilona Kuzmina
 Dr. Edgars Kviesis-Kipge
 Dr. Ilze Lihacova
 Dr. Uldis Rubins
 MSc. Inga Shirante

SUNDAY 27 August

Museum Hall, 4th floor, Raina Blvd. 19

16:00 Registration and poster set-up

17:00 Welcome Reception and Poster Session

MONDAY 28 August

Auditorium #13, 3rd floor, Raina Blvd. 19

8:30 Registration

Optical Clinical Diagnostics

9.00 – 9.30 PLENARY PRESENTATION

9:00 V. Tuchin (RU). Tissue Immersion Clearing for Enhanced Imaging within the Ultra-Broad Wavelength Range: from Free Electrons to Optical and Terahertz Waves.

9:30 – 10.30 INVITED PRESENTATIONS

9:30 E. Borisova (BG). Microscopic and Macroscopic Spectral Peculiarities of Cutaneous Tumours

9:50 M. Jędrzejewska-Szczerska (PL). Low-Coherence Interferometric Fiber-Optic Sensors with Potential Applications as Biosensors

10:10 I. Meglinski (FI). Combined Structured Muller-Matrix Imaging of Turbid Optically Anisotropic Tissue-Like Scattering Medium with a Purpose of Non-Invasive Cancer Diagnosis

10:30 Coffee break

11.00 – 12.20 ORAL PRESENTATIONS

11:00 G. Revalde, K. Grundšteins, J. Alnis, A. Skudra. Cavity Ring down Spectrometry for Disease Diagnostics Using Exhaled Air

11:20 M. S. Wróbel, S. Siddhanta, J. Smulko, I. Barman. Surface-enhanced Raman Spectroscopy for Detection of Drugs in Blood

11:40 A. Tereshchenko, V. Fedorenko, V. Smyntyna, I. Konup, A. Konup, M. Eriksson, R.Y. akimova, S. Balme, M. Bechelany, A. Ramanavicius. Towards Immunosensor for the Determination of GVA-Antigen Based on Photoluminescence of ZnO Films

12:00 K. Karpienko, M. Wąsowicz, M. Ficek, M. Jędrzejewska-Szczerska. Optical Investigation of Nanodiamonds Interactions with Blood

12:20 Lunch

Optical In-vivo Monitoring

13.30 – 14.00 PLENARY PRESENTATION

13:30 A. Kamshilin (RU). Remote Photoplethysmography: Where Does the Signal Come From?

14.00 – 15.00 INVITED PRESENTATIONS

14:00 W. Verkruyse (NL). Recent Developments in Contactless Health Monitoring

14:20 U. Rubins (LV). Remote Photoplethysmography Technique for Monitoring of Regional Anesthesia Effectiveness

14:40 K. Wårdell (SE). Optical Techniques for Monitoring in Neurosurgery

15:00 *Coffee break*

15.30 – 16.50 ORAL PRESENTATIONS

15:30 M. Huotari, K. Määttä, J. Röning. PPG of Young and Elderly People, Clinical Patients, and Cohorts

15:50 Z. Marcinkevics, U. Rubins, A. Caica, E. Dislere, A. Grabovskis. Evaluation of Nitroglycerin Effect on Remote Photoplethysmogram Waveform

16:10 A. Lihachev, I. Lihacova, J. Spigulis, T. Trebst, M. Wehner. Monitoring Soft Tissue Coagulation by Optical Spectroscopy

16:30 M. Volynsky, R. Giniatullin, O. Mamontov, A. Kamshilin. Study of Capsaicin-induced Changes of Blood Circulation by Imaging Plethysmography

17:00 – 22:00 *Excursion, Conference Dinner*

TUESDAY 29 August

Auditorium #13, 3rd floor, Raina Blvd. 19

Biomedical Tissue Imaging

9.00 – 10.00 PLENARY PRESENTATIONS

9:00 S. Andersson-Engels (IE). Acousto-optics for Deep Tissue Imaging and Photo-manipulation

9:30 M. Niedre (USA). Fluorescence Detection of Rare Circulating Cells In Vivo: Technology, Applications and Future Prospects

10:00 – 10.40 INVITED PRESENTATIONS

10:00 G. Salerud (SE). Multispectral Snapshot Imaging to Record Spatial and Temporal Tissue Oxygenation Maps

10:20 R. Rotomskis (LT). Quantum Dots Accumulation and Distribution In Vivo with Special Reference to the Barriers between Different Tissues Species

10:40 *Coffee break*

11:00 – 12.20 ORAL PRESENTATIONS

11:00 B. Cugmas, F. Pernuš, B. Likar. Color Constancy in Dermatoscopy with Smartphone

11:20 D. Bliznuks, I. Kuzmina, K. Bolocko, A. Lihacovs. Image Quality Enhancement for Skin Cancer Optical Diagnostics

11:40 M. Iralieva, O. Myakinin, I. Bratchenko, V. Zakharov. Computer Simulation of Skin Dermoscopy Images

12:00 I. Lihacova, K. Bolocko, A. Lihachev. Semi-automated Non-invasive Diagnostics Method for Melanoma Differentiation from Nevi and Basal Cell Carcinomas

12:20 *Lunch*

Biophotonics Technology Trends

13:30 J. Spigulis. Introduction

14:00 Round table discussion – expert panel

16:00 *Closing*

POSTER PRESENTATIONS

1. I. Brice, A. Pirkina, A. Ubele, K. Grundsteins, A. Atvars, R. Viter, J. Alnis.
Development of Optical WGM Resonators for Biosensors.
2. I. Carneiro, S. Carvalho, R. Henrique, L. Oliveira, V. Tuchin.
Water Content in Human Liver from Dispersion Evaluation.
3. M. Galat, N. Shpyrka, M. Taran, O. Pareniuk, K. Shavanova, O. Boiko.
Toxoplasmosis Diagnostics Based on Photoluminescence of Zinc Oxide Nanoparticles.
4. D. Joseph. **Speckle Scattering Studies from Red Blood Cell Suspension.**
5. E. Konstantinova, A. Zyubin, V. Slezhkin, E. Moiseeva, K. Matveeva, V. Bryukhanov.
Application of Quantum Dots CdZnSeS/ZnS Luminescence, Enhanced by Plasmons of Roughness Silver Surface for Detection of Albumin in Blood Facies of Infected Person.
6. I. Kuzmina, E. Borisova, Ts. Genova, P. Troyanova, J. Spigulis.
Towards In Vivo Skin Cancer Detection by Colour Parameters.
7. I. Kuzmina, U. Rubins, I. Saknite, J. Spigulis.
Rosacea Assessment by Erythema Index and Principal Component Analysis Segmentation Maps.
8. E. N. Lazareva, P. A. Timoshina, D. K. Tuchina, V. I. Kochubey, A. B. Bucharskaya, D. A. Alexandrov, I. G. Samusev, N. A. Myslitskaya, V. V. Bryukhanov, V. V. Tuchin.
Refractometry and Fluorescence Spectroscopy of Hemoglobin from Whole Blood of Rats with Alloxan Diabetes.
9. A. Lihachev, E. V. Plorina, A. Derjabo, M. Lange, I. Lihacova.
Evaluation of Skin Pathologies by RGB Autofluorescence Imaging.
10. O. Polschikova, A. Machikhin, V. Batshev, A. Ramazanov, V. Pozhar.
Optical System of a Microscope Module for Multispectral Quantitative Phase Imaging Based on Acousto-optic Filtration of Light.
11. G. Revalde, K. Grundšteins, J. Alnis, A. Skudra.
First Results of Cavity Ring Down Signals from Exhaled Air.
12. Yu. Ruban, V. Illienko, N. Nesterova, O. Pareniuk, K. Shavanova.
Estimation of the Effect of Radionuclide Contamination on Vicia Sativa L. Induction of Chlorophyll Fluorescence Parameters using "Floratest" Optical Biosensor.
13. N. Shpyrka, Y. Ruban, O. Pareniuk, K. Shavanova.
The Immune Biosensor for Ochratoxin-A Detection Based on the Surface Plasmon Resonance Effect.
14. M. Tamošiūnas, N. Kuliešienė, R. Daugelavičius.
Implicit Dosimetry of Microorganism Photodynamic Inactivation.
15. M. Tamošiūnas, D. Jakovels, U. Rubins, J. Baltušnikas, R. Kadikis, R. Petrovskas, S. Šatkauskas.
pEGFP Transfection into Murine Skeletal Muscle by Electrosonoporation.
16. A. Zyubin, E. Konstantinova, V. Slezhkin, K. Matveeva, I. Samusev, V. Bryukhanov. **Application of Fluorescent and Vibration Spectroscopy for Septic Serum Human Albumin Structure Deformation during Pathology.**

PLENARY PRESENTATIONS	10
Valery V. Tuchin Tissue Immersion Clearing for Enhanced Imaging within the Ultra-Broad Wavelength Range: from Free Electrons to Optical and Terahertz Waves.....	10
Alexei A. Kamshilin Remote Photoplethysmography: Where Does the Signal Come From?	11
Jacqueline Gunther, Michael Raju and Stefan Andersson-Engels Acousto-optics for Deep Tissue Imaging and Photo-manipulation	12
Mark Niedre Fluorescence Detection of Rare Circulating Cells In Vivo: Technology, Applications and Future Prospects	13
INVITED PRESENTATIONS	14
E. Borisova, Ts. Genova, P. Troyanova, E. Pavlova, I. Terziev, N. Penkov, M. Lomova, D. Gorin, L. Avramov Microscopic and Macroscopic Spectral Peculiarities of Cutaneous Tumours	14
Małgorzata Jędrzejewska-Szczerska Low-Coherence Interferometric Fiber-Optic Sensors with Potential Applications as Biosensors	15
Igor Meglinski Combined Structured Muller-Matrix Imaging of Turbid Optically Anisotropic Tissue-Like Scattering Medium with a Purpose of Non-Invasive Cancer Diagnosis	16
Wim Verkruyse Recent Developments in Contactless Health Monitoring.....	17
U. Rubins, A. Miscuks, M. Lange, Z. Marcinkevics Remote Photoplethysmography Technique for Monitoring of Regional Anaesthesia Effectiveness	18
Karin Wårdell Optical Techniques for Monitoring in Neurosurgery.....	19
E. Göran Salerud, M. Larsson, M. Ewerlöf Multispectral Snapshot Imaging to Record Spatial and Temporal Tissue Oxygenation Maps.....	20
Ricardas Rotomskis Quantum Dots Accumulation and Distribution In Vivo with Special Reference to the Barriers between Different Tissues Species.....	21

ORAL PRESENTATIONS	22
G. Revalde, K. Grundšteins, J. Alnis, A. Skudra. Cavity Ring down Spectrometry for Disease Diagnostics Using Exhaled Air	22
M. S. Wróbel, S. Siddhanta, J. Smulko, I. Barman Surface-enhanced Raman Spectroscopy for Detection of Drugs in Blood	23
A. Tereshchenko, V. Fedorenko, V. Smyntyna, I. Konup, A. Konup, M. Eriksson, R. Yakimova, S. Balme, M. Bechelany, A. Ramanavicius Towards Immunosensor for the Determination of GVA-Antigen Based on Photoluminescence of ZnO Films	24
K. Karpjenko, M. Wąsowicz, M. Ficek, M. Jędrzejewska-Szczerska Optical Investigation of Nanodiamonds Interactions with Blood	25
M. Huotari, K. Määttä, J. Rönig PPG of Young and Elderly People, Clinical Patients, and Cohorts	26
Z. Marcinkevics, U. Rubins, A. Caica, E. Dislere, A. Grabovskis Evaluation of Nitroglycerin Effect on Remote Photoplethysmogram Waveform	27
A. Lihachev, I. Lihacova, J. Spigulis, T. Trebst, M. Wehner Monitoring Soft Tissue Coagulation by Optical Spectroscopy	28
M. Volynsky, R. Giniatullin, O. Mamontov, A. Kamshilin Study of Capsaicin-induced Changes of Blood Circulation by Imaging Plethysmography	29
B. Cugmas, F. Pernuš, B. Likar Color Constancy in Dermatoscopy with Smartphone	30
D. Bliznuks, I. Kuzmina, K. Bolocko, A. Lihacovs Image Quality Enhancement for Skin Cancer Optical Diagnostics	31
M. Iralieva, O. Myakinin, I. Bratchenko, V. Zakharov Computer Simulation of Skin Dermoscopy Images	32
I. Lihacova, K. Bolocko, A. Lihachev Semi-automated Non-invasive Diagnostics Method for Melanoma Differentiation from Nevi and Basal Cell Carcinomas	33
POSTER PRESENTATIONS	34
I. Brice, A. Pirkatina, A. Ubele, K. Grundsteins, A. Atvars, R. Viter, J. Alnis Development of Optical WGM Resonators for Biosensors	34
I. Carneiro, S. Carvalho, R. Henrique, L. Oliveira, V. Tuchin Water Content in Human Liver from Dispersion Evaluation	35
M. Galat, N. Shpyrka, M. Taran, O. Pareniuk, K. Shavanova, O. Boiko Toxoplasmosis Diagnostics Based on Photoluminescence of Zinc Oxide Nanoparticles	36
David Joseph Speckle Scattering Studies from Red Blood Cell Suspension	37

E. Konstantinova, A. Zyubin, V. Slezhkin, E. Moiseeva, K. Matveeva, V. Bryukhanov Application of Quantum Dots CdZnSeS/ZnS Luminescence, Enhanced by Plasmons of Roughness Silver Surface for Detection of Albumin in Blood Facies of Infected Person	38
I. Kuzmina, E. Borisova, Ts. Genova, P. Troyanova, J. Spigulis Towards In Vivo Skin Cancer Detection by Colour Parameters	39
I. Kuzmina, U. Rubins, I. Saknite, J. Spigulis Rosacea Assessment by Erythema Index and Principal Component Analysis Segmentation Maps	40
E. N. Lazareva, P. A. Timoshina, D. K. Tuchina, V. I. Kochubey, A. B. Bucharskaya, D. A. Alexandrov, I. G. Samusev, N. A. Myslitskaya, V. V. Bryukhanov, V. V. Tuchin Refractometry and Fluorescence Spectroscopy of Hemoglobin from Whole Blood of Rats with Alloxan Diabetes	41
A. Lihachev, E. V. Plorina, A. Derjabo, M. Lange, I. Lihacova Evaluation of Skin Pathologies by RGB Autofluorescence Imaging	42
O. Polschikova, A. Machikhin, V. Batshev, A. Ramazanova, V. Pozhar Optical System of a Microscope Module for Multispectral Quantitative Phase Imaging Based on Acousto-optic Filtration of Light	43
G. Revalde, K. Grundšteins, J. Alnis, A. Skudra First Results of Cavity Ring down Signals from Exhaled Air	44
Yu. Ruban, V. Il'ienko, N. Nesterova, O. Pareniuk, K. Shavanova Estimation of the Effect of Radionuclide Contamination on Vicia Sativa L. Induction of Chlorophyll Fluorescence Parameters Using "Floratest" Optical Biosensor	45
N. Shpyrka, Y. Ruban, O. Pareniuk, K. Shavanova The Immune Biosensor for Ochratoxin-A Detection Based on the Surface Plasmon Resonance Effect	46
M. Tamošiūnas, N. Kuliešienė, R. Daugelavičius Implicit Dosimetry of Microorganism Photodynamic Inactivation	47
M. Tamošiūnas, D. Jakovels, U. Rubins, J. Baltušnikas, R. Kadikis, R. Petrovskas, S. Šatkauskas pEGFP Transfection into Murine Skeletal Muscle by Electrosonoporation	48
A. Zyubin, E. Konstantinova, V. Slezhkin, K. Matveeva, I. Samusev, V. Bryukhanov Application of Fluorescent and Vibration Spectroscopy for Septic Serum Human Albumin Structure Deformation during Pathology	49

Tissue Immersion Clearing for Enhanced Imaging within the Ultra-Broad Wavelength Range: from Free Electrons to Optical and Terahertz Waves

Valery V. Tuchin

Saratov National Research State University, Saratov, Russia
Institute of Precision Mechanics and Control RAS, Saratov, Russia
National Research Tomsk State University, Tomsk, Russia

E-mail: tuchinvv@mail.ru

Immersion clearing/contrasting technique is aiming to enhance imaging of living tissues by using different imaging modalities working in an ultra-broad wavelength range from free electron beam excitation (Cherenkov light emission) to terahertz waves. The method is based on controllable and reversible modification of tissue properties by their impregnation with a biocompatible clearing/contrasting agent (CCA). The basis of innovative recently proposed multimodal diagnostic medical technologies with the targeting by a unified CCA (THz/optical, x-ray/optical, MRT/optical) will be discussed. Water transport and modification of tissue mechanical properties under CCA action such as reversible dehydration and shrinkage, balance of free and bound water will be analyzed.

The enhancement of probing depth and image contrast for different human and animal tissues will be demonstrated using diffuse spectroscopy, OCT, photoacoustic microscopy, linear and nonlinear fluorescence, SHG and Raman microscopies, polarization and speckle imaging. Perspectives of application of immersion optical clearing method to improve weak luminescence from upconversion nanoparticles deeply inserted into living tissue and to detect Cherenkov's fluorescence excited by free electrons or protons in tissue depth will be discussed. Experimental data on diffusivity and permeability of glucose, glycerol, PEG, Omnipaque™ (x-ray contrast) and other clearing agents applied to normal and pathological tissues will be presented.

- [1] D. Zhu, et al., "Recent progress in tissue optical clearing," *Laser Photonics Rev.* 7(5), 732–757 (2013).
- [2] V. V. Tuchin, "In vivo optical flow cytometry and cell imaging," *Rivista Del Nuovo Cimento*, 37(7), 375–416 (2014).
- [3] E. A. Genina, et al., "Optical clearing of biological tissues: prospects of application in medical diagnostics and phototherapy [Review]," *J. Biomed. Photonics & Eng.* 1(1), 22–58 (2015).
- [4] V. V. Tuchin, "Tissue optical clearing: New prospects in optical imaging and therapy," in *BioPhotonics, IEEE International Conference*, pp.1–10, 20–22 May 2015; doi: 10.1109/BioPhotonics.2015.7304023.
- [5] V. V. Tuchin, "Polarized light interaction with tissues," *J. Biomed. Opt.* 21(7), 071114–1–37 (2016)

Remote Photoplethysmography: Where Does the Signal Come From?

Alexei A. Kamshilin

ITMO University, St. Petersburg, Russia
E-mail: alexei.kamshilin@yandex.ru

Photoplethysmography is a simple and low-cost measuring technique which can provide valuable information about the cardiovascular system [1]. Recently, remote photoplethysmography (rPPG) was introduced as a technique for distant measurement and monitoring of physiological signals related to the cardiac activity [2,3]. It is based on the data processing of conventional video recordings of a selected body's part illuminated by incoherent visible light. In spite of the long history of photoplethysmography, the mechanism of light interaction with pulsatile blood vessels is still a subject of continuing debates. The classical model assumes that the PPG waveform mainly originates from the heart-driven changes of blood volume in major blood vessels, which modulate the light absorption [1]. In contrast, recent alternative model suggests the light to be modulated due to compression/decompression of the capillary bed provided by changes of blood pressure in deep vessels located nearby the measuring place [4].

To support the new alternative model of light interaction with living tissue we will discuss several experimental observations, which are hardly explained in the frames of the classical PPG model. Among these observations are influence of the skin status on the amplitude of light modulation [5]; confirmation of absence of blood pulsations at the heartbeat frequency in capillaries by video microscopy diameter [6]; and significant change of the reflected light intensity caused by blood filling of a forearm during the venous occlusion [7]. Correct interpretation of the plethysmography signals is very important since it could be used for development of novel applications of this simple and cost-efficient technique in biology and medicine.

Financial support provided by the Russian Science Foundation (grant 15-15-20012) is acknowledged.

- [1] J. Allen, "Photoplethysmography and its application in clinical physiological measurement," *Physiol. Meas.* 28, R1–R39 (2007).
- [2] F. P. Wieringa, et al., "Contactless multiple wavelength photoplethysmographic imaging: a first step toward "SpO2 camera" technology," *Ann. Biomed. Eng.* 33, 1034–1041 (2005).
- [3] W. Verkrusse, et al., "Remote plethysmographic imaging using ambient light," *Opt. Express* 16, 21434–21445 (2008).
- [4] A. A. Kamshilin, et al., "A new look at the essence of the imaging photoplethysmography," *Sci. Rep.* 5, 10494 (2015).
- [5] A. A. Kamshilin, et al., "Influence of skin status on the light interaction with dermis," *Biomed. Opt. Express* 6, 4326–4334 (2015).
- [6] M. A. Volynsky, et al., "Blood peripheral circulation assessment method based on combined use of the video-capillaroscopy, imaging photoplethysmography, and electrocardiography," (*Optical Society of America, Heidelberg, Germany*, 2016), p. JT3A.26; doi: 10.1364/3D.2016.JT3A.26.
- [7] A. A. Kamshilin, et al., "Novel contactless approach for assessment of venous occlusion plethysmography by video recordings at the green illumination," *Sci. Rep.* 7, 464 (2017).

Acousto-optics for Deep Tissue Imaging and Photo-manipulation

Jacqueline Gunther¹, Michael Raju¹ and Stefan Andersson-Engels^{1,2}

¹IPIC, Tyndall National Institute, Cork, Ireland

²Department of Physics, University College Cork, Cork, Ireland

E-mail: stefan.andersson-engels@tyndall.ie

The newly established Biophotonics@Tyndall team has an aim to improve patient care by develop and deploy biophotonics methods for medical use. We aim to be active both in clinical and industrial translation as in more fundamental long term, high-impact research. Acousto-optical tomography (AOT) has a potential to provide molecular contrast information at many centimeters in tissue with tenths of micrometers resolution. The presentation will include a review of the AOT field. It will also include simulation results. The signal contrast-to-noise ratio (CNR) was modeled using Monte Carlo simulations both in reflection and transmission geometries. The target volume contrast in absorption was 50%. In the reflection geometry (using a source-detector distance of 4 cm) the CNR was >1 for depths down to 4.75 cm, while all depths showed a CNR>1 for a 10 cm thick tissue slab.

Optical imaging of biological tissue has good molecular contrast but poor penetration depth beyond the very superficial tissue. For deep locations it also provides poor spatial resolution. This is the case even using more deeply penetrating near infrared light under optimal conditions. Acousto-optical tomography combines the spatial resolution of ultrasound imaging with the contrast of optical imaging. How deeply it can measure is still not fully understood, and will be investigated in this work. In AOT one sends light through an ultrasound focus in a medium, where the light become frequency shifted or "tagged" through a process described by the acousto-optic effect.

In this study, a single Monte Carlo (MC) simulation was run using a CUDAMCML code assuming a semi-infinite medium. Beam convolution was performed in a custom made program in MatLab using the procedures developed by Wang et. al. for the conventionally used MCML code. The parameters used in the MC simulation were 10^9 photon packets launched into a medium. The optical properties of the medium was $\mu_a = 0.2 \text{ cm}^{-1}$, $\mu_s = 50 \text{ cm}^{-1}$, $g = 0.9$, and $n = 1.37$; for the absorption, scattering, anisotropy and refractive index, respectively. The MC simulation yielded a map of the light fluence rate in the semi-infinite medium modeled. This map was used for all convolutions and calculations needed to calculate the final CNR. For these calculations an energy of 0.5 J was considered during a 250 ms light pulse, meeting the laser safety limits. The CNR was found to be in excess of 1 for any depth smaller than 4.75 cm using the reflectance geometry. The performance of the technique was also in the transmission geometry for medium lengths of 4 cm, 6 cm, 8 cm, and 10 cm. For each of these lengths, the CNR decreases close to the front and rear surfaces of the medium, while it remains more or less constant at all depths further from the surface. As the length of the medium increases the CNR decreased. Furthermore, the 8 cm slab had a CNR>10 at all imaging depth for objects with $\mu_a = 0.3 \text{ cm}^{-1}$. Also, a CNR of above 1 was found for all depths of the 10 cm slab medium.

In summary, the results suggest AOT will be able to study tissue deeply located inhomogeneities in tissue. They indicate it is possible to image an inclusion down to about 5 cm in a reflection geometry and within a 10 cm slab in the transmission geometry.

ACKNOWLEDGEMENTS

This research was supported by Science Foundation Ireland. We kindly acknowledge the interesting discussions with Stefan Kröll, Andreas Walther, Lars Rippe and Lihong Wang.

Fluorescence Detection of Rare Circulating Cells In Vivo: Technology, Applications and Future Prospects

Mark Niedre

Northeastern University, Boston, MA, USA

Email: m.niedre@neu.edu

Many important biological processes and diseases involve circulating cells in the bloodstream. For example, cancer metastasis is mediated by the dissemination of circulating tumour cells (CTCs) via the blood. As such, study of CTCs is of great interest in pre-clinical and clinical research. Most methods involve removal, purification and analysis of small blood samples. However, it has been shown that these methods frequently yield count errors, miss rare cell populations entirely, and in the case of animal models may induce an undesired inflammatory processes.

In contrast, "in vivo flow cytometry" allows non-invasive and continuous optical detection of circulating cells directly in the bloodstream. Our group has a particular interest in developing technologies for fluorescence detection of rare circulating cells, specifically fewer than 100 cells per mL of blood. Rare cells are critical in cancer metastasis, and yet are difficult to detect with microscopy-based methods. In this talk, I will first discuss our technology – "Diffuse in vivo Flow Cytometry" (DiFC) – which uses diffuse photons to sample relatively large circulating blood volumes. Through use of careful optical design, electronic filtering and signal processing approaches, we are able to detect and enumerate individual rare circulating cells in bulk tissue. I will also discuss applications of DiFC in the basic study of disease development, response to new treatments, and potentially ultimately in humans.

Microscopic and Macroscopic Spectral Peculiarities of Cutaneous Tumours

**E. Borisova¹, Ts. Genova¹, P. Troyanova², E. Pavlova²,
I. Terziev², N. Penkov², M. Lomova³, D. Gorin³, L. Avramov¹**

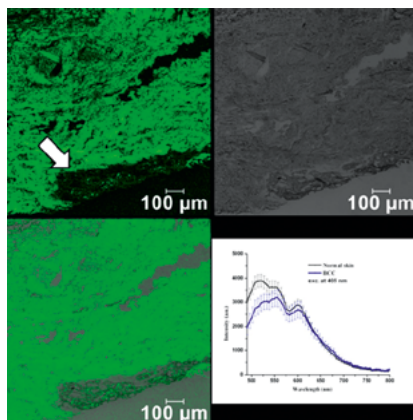
¹ Biophotonics lab., Institute of Electronics, Bulgarian Academy of Sciences, Sofia, Bulgaria

² University Hospital "Tzaritza Yoanna-ISUL", Sofia, Bulgaria

³ Nano- and Biomedical Technologies Department, Saratov State University, Saratov, Russia

E-mail: borisova@ie.bas.bg

Autofluorescence spectral and confocal microscopic measurements were made on different cutaneous neoplastic lesions, namely basal cell carcinoma, squamous cell carcinoma, malignant melanoma, and their dysplastic forms – keratoacantoma, dysplastic nevi and benign lesions related – basal cell papiloma, seboreic keratosis and compound nevi using excitation at 405 nm.



Confocal fluorescent (left) and optical (right) microscopy images of basal cell carcinoma stained histological sample and autofluorescence spectra of normal and basal cell carcinoma lesion in vivo; excitation at 405 nm for microscopic and spectroscopic measurements is applied.

Spectroscopic investigations were made on in vivo and ex vivo tissue samples, and confocal microscopy investigations were made on ex vivo and eosin-haematoxylin stained thin slices of the tumours detected. Specific spectral features observed in each type of lesion investigated on micro and macro level would be presented and discussed. Correlation between the spectral data received and the microscopic features observed would be discussed in the report.

ACKNOWLEDGEMENTS

This work is supported in part by the National Science Fund of Bulgarian Ministry of Education and Science under grant #DFNI-B02/9/2014 "Development of biophotonics methods as a basis of oncology theranostics", and in part under COST Action BM1205 "European Network for Skin Cancer Detection Using Laser Imaging".

Low-Coherence Interferometric Fiber-Optic Sensors with Potential Applications as Biosensors

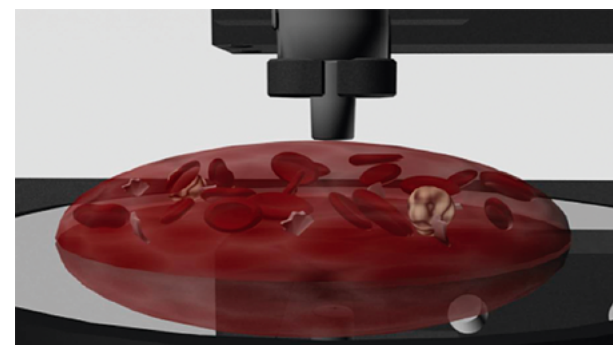
Małgorzata Jędrzejewska-Szczerska

Department of Metrology and Optoelectronics,
Gdańsk University of Technology, Gdańsk, Poland

E-mail: mjedrzej@eti.pg.gda.pl

Low-coherence sensors using are finding new applications in biophotonic sensing, especially using new materials made available by the technological progress. The nanolayers made from the new materials such as: nanodiamond (NCD), boron-doped nanodiamond (B-NCD), zinc oxide (ZnO), titanium dioxide (TiO₂) have been used in the construction of low coherence sensors in fiber-optic configuration. They can be used as protective coating, reflective layer and as a sensing medium. Nanodiamond and boron-doped nanodiamond have been made by the Chemical Vapor Deposition (CVD), hence metallic based layers were deposited in the Atomic Layer Deposition Process.

The configuration of a few fiber-optic low coherence sensors using nanolayers has been design and their ability to perform biophotonic measurements was conducted.



The sensor head of low-coherent interferometric fiber-optic sensor

[1] Hirsch M. et al. "Application of TiO₂ thin film in low-coherence fiber-optic biosensors", *Sensors* 17(2), 261 (2017).
[2] Majchrowicz D. et al. "Application of Thin ZnO ALD Layers in Fiber-Optic Fabry-Pérot Sensing Interferometers", *Sensors* 16(3), 416 (2016).

[3] Milewska D. et al. "Application of thin diamond films in low-coherence fiber-optic Fabry-Pérot displacement sensor", *Diamond and Related Materials* 64 (2016).

[4] Jędrzejewska-Szczerska M., "Response of a New Low-Coherence Fabry-Pérot Sensor to Hematocrit Levels in Human Blood", *SENSORS*, 14(4), 6965-6976. (2014).

[5] Jędrzejewska-Szczerska M. et al., "ALD thin ZnO layer as an active medium in a fiber-optic Fabry-Pérot interferometer", *Sensors and Actuators A – Physical*, 221, 88-94. (2015).

[6] Karpienko K. et al., "Blood equivalent phantom vs. whole human blood, a comparative study", *Journal of Innovative Optical Health Science*, 9(5), 1650012-1-9. (2016)

Combined Structured Muller-Matrix Imaging of Turbid Optically Anisotropic Tissue-Like Scattering Medium with a Purpose of Non-Invasive Cancer Diagnosis

Igor Meglinski

Optoelectronics and Measurement Techniques Laboratory,
University of Oulu, P.O. Box 4500, Oulu, 90014 Finland

E-mail: igor.meglinski@oulu.fi

The Mueller-matrix (MM) polarimetry is extensively used for characterization of optically anisotropic highly scattering biological tissues, including cancerous samples. We introduce a combined structured analysis of the MM images of optically anisotropic turbid tissue-like scattering media and biological samples. We demonstrate that a combined use of statistical, correlational and fractal approaches for analysis of polarization-inhomogeneous fields observed in case of screening multiple-scattering biological tissues is an effective tool for diagnosis of variations in optical anisotropy due to oncological changes. The obtained results suggest a high potential of MM polarimetry in clinical application for diagnosis and quantitative characterization of thick highly scattering biological tissues.

Recent Developments in Contactless Health Monitoring

Wim Verkruysse

Philips Research Standardization Research & Robust Sensing,
Eindhoven, the Netherlands

E-mail: wim.verkruysse@philips.com

Scientific interest in contactless health monitoring has increased dramatically over the past years with the recognition that cameras can not only be used for tele-monitoring patient presence and activity, but also measure vital signs such as respiration rate, pulse rate [1,2] and even SpO₂, the arterial oxygen saturation [3,4]. In particular patients with fragile skin, such as premature neonates would benefit if cameras could monitor them satisfactorily in an entirely contactless manner [5].

The measurement of pulse and SpO₂ uses photo-plethysmography (PPG) which is the underlying principle for pulse-oximetry. Even though the principle is the same in camera based PPG, illumination and detection geometry are considerably different, which raises questions on the origin of the signal [6] and calibrability of SpO₂, if the PPG signal is not (only) originating in the arterioles, as in conventional pulse-oximetry.

Besides this fundamental question, a more practical but challenging question needs to be addressed. Contactless health monitoring only has a future if patient motion can be addressed [7]. In camera based pulse-oximetry, patient motion can be more severe than in contact probes while the PPG signal is orders of magnitude smaller.

Recent progress addressing these fundamental [4] as well as practical questions [8] will be shown. Results will be shown for both healthy volunteers in laboratory conditions and premature infants in the neonatal intensive care unit.

Finally, an outlook on a very exciting additional feature, offered by camera based PPG, is provided. Besides 1-dimensional signals, such as pulse and SpO₂, PPG imaging [9-11] is likely to provide new insights in patient well-being and further accelerate the development of contactless health monitoring.

[1] C. Takano, et al. "Heart rate measurement based on a time-lapse image." Medical engineering & physics 29(8), 853-857 (2007).

[2] W. Verkruysse, et al. "Remote plethysmographic imaging using ambient light." Optics Express 16(26), 21434-21445 (2008).

[3] F. Wieringa, et al. "Contactless multiple wavelength photoplethysmographic imaging: a first step toward "SpO₂ camera" technology." Annals of biomedical engineering 33(8) 1034-1041 (2005).

[4] W. Verkruysse, et al. "Calibration of contactless pulse oximetry." Anesthesia and analgesia 124(1) 136 (2017).

[5] L. Aarts, et al. "Non-contact heart rate monitoring utilizing camera photoplethysmography in the neonatal intensive care unit- a pilot study." Early human development 89(12), 943-948 (2013).

[6] A. Kamshilin, et al. "A new look at the essence of the imaging photoplethysmography." Scientific reports 5 10494 (2015).

[7] G. De Haan, et al. "Improved motion robustness of remote-PPG by using the blood volume pulse signature." Physiological measurement 35(9), 1913 (2014).

[8] M. van Gastel, et al. "New principle for measuring arterial blood oxygenation, enabling motion-robust remote monitoring." Scientific Reports 6 (2016).

[9] A. Moço, et al. "Ballistocardiographic artifacts in PPG imaging." IEEE Transactions on Biomedical Engineering 63(9) 1804-1811 (2016).

[10] Kamshilin, Alexei A., et al. "Photoplethysmographic imaging of high spatial resolution." Biomedical optics express 2(4), 996-1006 (2011).

[11] U. Rubins, et al. "Real-time photoplethysmography imaging system." 15th Nordic-Baltic Conference on BME and Medical Physics (NBC 2011). Springer Berlin Heidelberg, 2011.

Remote Photoplethysmography Technique for Monitoring of Regional Anaesthesia Effectiveness

U. Rubins¹, A. Miscuks², M. Lange¹, Z. Marcinkevics³

¹Institute of Atomic Physics and Spectroscopy, University of Latvia, Riga, Latvia

²Hospital of Traumatology and Orthopedics, Riga, Latvia

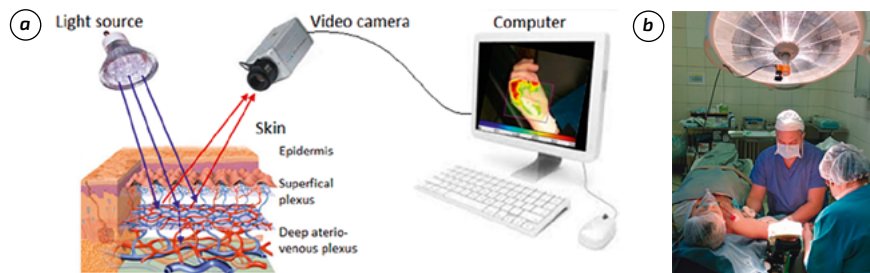
³Department of Human and Animal Physiology, University of Latvia, Riga, Latvia

E-mail: uldisrubins@yahoo.com

Remote photoplethysmography (rPPG) is a non-contact optical diagnostic technique for detecting blood volume changes in the microvascular bed of tissue [1-3]. Contactless rPPG monitoring has advantages in cases when the skin blood microcirculation should be detected remotely in sterile conditions, e.g. for surgery feedback control, burn monitoring or monitoring of newborns.

Previously our group developed rPPG prototype systems for mapping of palm skin microcirculation during the regional anesthesia (RA) manipulations [1-2]. In the case of peripheral block of plexus brachialis, the local anesthetic affects four different nerves, and subsequent microcirculation changes of four different skin zones (dermatomes) can be observed. To ensure that the RA procedure is correct, it is important to immediately detect the effect of local anesthetic in each dermatome during the manipulation.

The developed rPPG system involves compact video camera, equipped with optical band-pass filter (520-580nm), which is adapted for handle attachment on the surgical lamp. The camera is connected to laptop computer. Our developed rPPG analysis algorithm involves automated recognition of hand palm, segmentation of palm image and rPPG amplitude visualization in several palm zones (fingers and palm body). The algorithm was implemented in Matlab GUI software. The rPPG software can process 100 fps video in real-time to obtain high-resolution rPPG amplitude maps. The modified Eulerian-based algorithm [3] showed good compromise solution for sensitivity and spatial resolution of rPPG amplitude maps for 2-D visualization of palm microcirculation.



The principle of rPPG technique (a) and monitoring of regional anesthesia by means of rPPG (b)

[1] U. Rubins, J. Spigulis, A. Miscuks. Photoplethysmography imaging algorithm for continuous monitoring of regional anesthesia. ESTIMedia'16 Proc. of 14th ACM/IEEE Symposium on Embedded Systems for Real-Time Multimedia, pp. 67-71 (2016).

[2] J. Spigulis. Biophotonic technologies for non-invasive assessment of skin condition and blood microcirculation. Latv. J. Phys. Tech. Sci. 49(5), 63 (2012).

[3] H. Wu, M. Rubinstein, E. Shih, J. Guttat, F. Durand, W. T. Freeman. Eulerian Video Magnification for Revealing Subtle Changes in the World. ACM Trans. on Graphics, 31(4) (Proc. SIGGRAPH) (2012)

Optical Techniques for Monitoring in Neurosurgery

Karin Wårdell

Department of Biomedical Engineering, Linköping University, Linköping Sweden

E-mail: karin.wardell@liu.se

During the last decade the interest for using optical techniques in monitoring of cerebral tissue parameters has increased. A review [1] of methods developed and implemented for neurosurgical use will be presented. We are presently working along three lines: I) Optical navigational tools for stereotactic implantation of deep brain stimulation (DBS) leads. A rigid guide with optical fibres is used for creation of the DBS-lead trajectory. It has been evaluated in more than 120 DBS implantations. It's forward looking feature uses laser Doppler flowmetry (LDF) for detection of increased blood flow, and thus help reduce the risk for haemorrhage. LDF also distinguish between grey-white tissue boundaries [2]. The same guide can also estimate SO₂ through processing of reflectance spectroscopy data [3]. II) The neurosurgical microscopes are today available with filters for several wavelengths. The blue light microscope is suitable for enhancement of malignant tumours by means of 5-aminolevulinic acid (ALA) induced fluorescence [4]. We have previously developed a hand-held probe fluorescence monitoring system. It has been used in more than 50 brain tumour resections of which about half together with the microscope. The performance of the probe system has been compared with fluorescence microscopy and biopsies. The results show that the probe system is superior in detecting weak fluorescence when using the recommended microscopy-dose of ALA (20mg/kg) [5]. Simultaneous recordings with the two systems are done without interference and problems with surrounding light. III) The third area applies optical methods for monitoring of cerebral microvascular blood flow during neuro-intensive care. A flexible probe and software for creating of trend curves based on LDF data has been designed. The system has been applied successfully in a four day long monitoring session on a patient treated for subarachnoid hemorrhage [6]. Further clinical studies are required to evaluate the optical systems' potential for assessing the onset of secondary brain injury. In conclusion, optical monitoring methods has already proven useful in neurosurgery, but further evaluation of the respective techniques' clinical performances is necessary.

[1] K. Wårdell, "Optical Monitoring Techniques for Navigation during Stereotactic Neurosurgery," Sensors and Materials, vol. 28, pp. 1105-1116, 2016.

[2] K. Wårdell, P. Zsigmond, J. Richter, and S. Hemm, "Relationship between laser Doppler signals and anatomy during deep brain stimulation electrode implantation toward the ventral intermediate nucleus and subthalamic nucleus," Neurosurgery, vol. 72, pp. ons127-40, Jun 2013.

[3] P. Rejmstad, P. Zsigmond, and K. Wårdell, "Oxygen Saturation Estimation in Brain Tissue using Diffuse Reflectance Spectroscopy along Stereotactic Trajectories," Optics Express, vol. 25, No. 7, pp. 1-10, 2017.

[4] W. Stummer, U. Pichlmeier, T. Meinel, O. D. Wiestler, F. Zanella, and H. J. Reulen, "Fluorescence-guided surgery with 5-aminolevulinic acid for resection of malignant glioma: a randomised controlled multicentre phase III trial," Lancet Oncol, vol. 7, pp. 392-401, May 2006.

[5] J. Richter, N. Haj-Hosseini, M. Hallbeck, and K. Wårdell, "Combination of Hand-Held Probe and Microscopy for Fluorescence Guided Surgery in the Brain Tumor Marginal Zone," Photodiagnosis Photodyn Ther, Feb 18 2017.

[6] P. Rejmstad, N. Haj-Hosseini, P. Oscar Åneman, and K. Wårdell, "Optical monitoring of cerebral microcirculation in neurointensive care," Submitted, 2017.

Multispectral Snapshot Imaging to Record Spatial and Temporal Tissue Oxygenation Maps

E. Göran Salerud, M. Larsson, M. Ewerlöf

Dept Biomedical Engineering Linköping University, Linköping, Sweden

E-mail: goran.salerud@liu.se

The oxygenation of living tissue is a fundamental parameter to evaluate the homeostasis of cells and tissue [1,2]. Clinically, visual observations of skin colour variations, as a reaction to provocation, can be used to indirectly assess the microcirculatory blood perfusion and oxygenation[3], temporally and spatially. Visual assessment utilize knowledge about the unique and well-defined light absorbing properties of haemoglobin, a chromophore found in red blood cells, where the degree of oxygen saturation[4] is reflected in different haemoglobin spectral signatures. Standard diffuse reflectance spectroscopy (DRS) [5] utilize optical fibres probes with a well-defined distance between sending and receiving fibres to more objectively asses in real time the oxygen saturation. HSI oximeters often use a liquid-crystal tuneable filter [6], an acousto-optic tuneable filter or mechanically adjustable filter wheels, which has too long response/switching times to monitor tissue hemodynamic. We use a snapshot imager, the xiSpec camera (MQ022HG-IM-SM4X4-VIS, XIMEA®), having 16 wavelength-specific Fabry–Perot filters overlaid on the custom CMOS-chip (IMEC) to estimate skin blood volume and oxygen saturation with high temporal and spatial resolution.

The spectral distribution of the bands is however substantially overlapping, which needs to be taken into account for an accurate. An inverse Monte Carlo analysis is performed using a two-layered skin tissue model, defined by epidermal thickness, haemoglobin concentration and oxygen saturation, melanin concentration and spectrally dependent reduced-scattering coefficient, all parameters relevant for human skin. The analysis takes into account the spectral detector response of the xiSpec camera. At each spatial location in the field-of-view, we compare the simulated output to the detected diffusively backscattered spectra to find the best fit. The imager is evaluated for spatial and temporal variations during arterial and venous occlusion protocols applied to the forearm. Estimated blood volume changes and oxygenation maps at 512x272 pixels show values that are comparable to reference measurements performed in contact with the skin tissue.

We conclude that the snapshot xiSpec camera, paired with an inverse Monte Carlo algorithm, permits us to use this sensor for spatial and temporal measurement of varying physiological parameters, such as skin tissue blood volume and oxygenation.

Quantum Dots Accumulation and Distribution In Vivo with Special Reference to the Barriers between Different Tissues Species

Ricardas Rotomskis

Biomedical physics laboratory, National Cancer Institute, Vilnius, Lithuania

E-mail: ricardas.rotomskis@nvi.lt

Due to their size, nanoparticles (NP) exhibit new physicochemical properties which are not prominent in their bulk materials and they have become important probes for biomedical applications as contrast agents, therapeutic compounds, drug delivery platforms and multi-functional particles. However the pattern of NP biodistribution, penetration through the protective biological barriers, and interaction with biomolecules are different from conventional organic drugs and contrast agents. Therefore the questions of NP biodistribution and biological effects are highly important for clinical applications as well as solving nanotoxicological issues. The beneficial as well as potential harmful effects of NP, first of all depend on their localization in the tissues and cells. Nevertheless, the mechanisms of NP translocation in the body, as of yet, are poorly described.

Quantum dots (QD) are semiconductor NP, 1-10 nm in size which exhibit the exceptional optical properties (stable and bright photoluminescence, size tunable spectroscopic properties, photostability, high photoluminescence quantum yield, high absorption, etc.) which make them ideal candidate for the fluorescence imaging applications. The surface of QD can be chemically modified with various organic ligands to obtain specific biological functionality. These properties enable QD to be used as a universal model for studying penetration of inorganic NP through tissues.

There are several barriers which have to be passed through by QD in order to distribute in organism. The primary barrier for external NP is the epithelium, which forms superficial layer of skin and line all internal tracts (gastrointestinal, respiratory, genitourinary, etc.). The ability of QD to penetrate through the blood vessels is one of the major factors determining NP distribution in the organism and it plays important role in biomedical applications. The main attention will be paid on the investigations of the mechanisms of active transport QD through the capillaries, migration and distribution in the tissues of experimental animals (CDF1 mice) by the confocal fluorescence microscopy.

The fluorescence microscopy was performed using a Nikon C1si confocal laser scanning fluorescence microscope (objectives: x20/0.5 Plan Fluor, x60/1.4 Plan Apo VC oil). The standard RGB detector was coupled with a 500-590 nm band-pass filter for green, and a 620-750 nm band-pass filter for red channels. A 488 nm Ar⁺ ion laser was used for PL excitation. Image processing was performed using "ImageJ 1.45" software. QD localization in the tissues of experimental animals was evaluated in the unstained tissue specimens by analyzing strong red QD PL in the background of green tissue autofluorescence.

The QD penetration through tissues depends on the structure of the extracellular matrix. QD may adhere to the endothelium but they are not translocated through endothelium to the deeper layers of the vessel wall. QD diffuse in the areolar connective tissue of tunica adventitia, but they are unable to pass to the tunica media from the outer as well as the inner surface of this layer. The limited penetration through the vascular wall determines the retention of QD within the blood vessels without remarkable extravasation to the extracellular tissue fluids in most organs. Intravascular retention is a major factor affecting the biodistribution of QD in the organism and pharmacokinetic parameters. The specificity of QD diffusion in different tissues could be used in the diagnostics as a treatment of certain diseases which involve vascular wall damage. Specific QD diffusion in different tissues will be discussed.

[1] Ellis, C. G. et al., "The microcirculation as a functional system," *Critical Care*, 9, S3-S8 (2005).

[2] Intaglietta, M., Johnson, P. C., and Winslow, R. M., "Microvascular and tissue oxygen distribution," *Cardiovascular Research*, 32(4), 632-643 (1996).

[3] Alkawaz, M. H. et al., "The Correlation between Blood Oxygenation Effects and Human Emotion Towards Facial Skin Colour of Virtual Human," *3d Research*, 6(2), (2015).

[4] Zijlstra, W. G. et al., and Meeuwse-van der Roest, W. P., "Absorption spectra of human fetal and adult oxyhemoglobin, de-oxyhemoglobin, carboxyhemoglobin, and methemoglobin," *Clin Chem*, 37(9), 1633-8 (1991).

[5] Hernandez, S. E. et al., "Diffuse reflectance spectroscopy characterization of hemoglobin and intralipid solutions: in vitro measurements with continuous variation of absorption and scattering," *Journal of Biomedical Optics*, 14(3), (2009).

[6] Ewerlöf, M. et al. "Estimating skin blood saturation by selecting a subset of hyperspectral imaging data," *Imaging, Manipulation, and Analysis of Biomolecules, Cells, and Tissues XIII*, 9328, (2015).

Cavity Ring down Spectrometry for Disease Diagnostics Using Exhaled Air

G. Revalde^{1,2}, K. Grundšteins^{2,3}, J. Alnis³, A. Skudra³

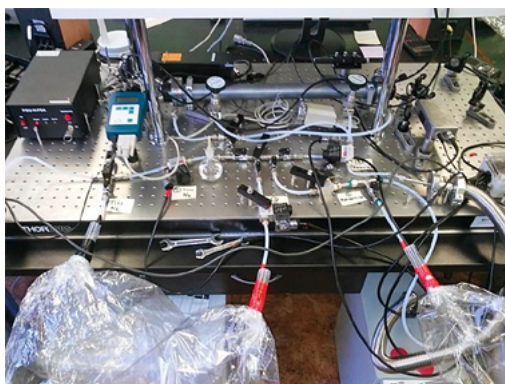
¹Institute of Technical Physics, Department of Material Science and Applied Chemistry, Rīga Technical University, Rīga, Latvia

²Smart Technology Centre, Ventspils University College, Ventspils, Latvia

³Institute of Atomic Physics and Spectrometry, University of Latvia, Rīga, Latvia

E-mail: gitar@latnet.lv

Cavity ring down spectrometry (CRDS) is a very sensitive spectrometric technique based on the absorption. We will report the development stage and first results of a cavity ring-down spectrometer system for the diagnostics of different diseases like diabetes and lung cancer using human breath analysis. Normal human breath contains many volatile organic compounds (VOC) in a very low concentration. Our CRDS is a portable system, placed on an optical breadboard [1]. The core part of the CRDS system is a resonator with high reflectivity mirrors at the both ends. We use pulsed Nd:Yag laser at 266 nm. A PMT and an oscilloscope register the CRDS signal. The concentration of VOC particles in the breath samples, let in in the resonator, is estimated from the exponential fit to the ring-down signal. First experiments allow us to determine acetone and benzene at the level below ppm. Breath samples from smokers are analysed.



Cavity ring-down spectrometer system for breath analysis.

ACKNOWLEDGEMENTS

G. Revalde and K. Grundšteins acknowledge the partial support from the National Research Programme "The next generation of information and communication technologies" (NexIT).

[1] G. Revalde et al, Cavity Ring-Down Spectroscopy measurements of Acetone concentration, IOP Conf. Series: Journal of Physics: Conf. Series 810 (2017) 012036.

Surface-enhanced Raman Spectroscopy for Detection of Drugs in Blood

M. S. Wróbel^{1,2}, S. Siddhanta¹, J. Smulko², I. Barman²

¹Department of Mechanical Engineering, Johns Hopkins University, Baltimore, MD 21218, USA

²Department of Metrology and Optoelectronics, Faculty of Electronics, Telecommunications and Informatics, Gdańsk University of Technology, Gdańsk, Poland

E-mail: maciejswrobel@gmail.com

We present a Surface-Enhanced Raman Spectroscopy approach for detection of drugs of abuse in whole human blood. We utilize a near infrared laser with 830 nm excitation wavelength in order to reduce the influence of fluorescence on the spectra of blood. However, regular plasmon resonance peak of plasmonic nanoparticles, such as silver or gold fall in a much lower wavelength regime about 400 nm. Therefore, we have shifted the plasmon resonance of nanoparticles to match that of an excitation laser wavelength, by fabrication of silver-core gold-shell nanoparticles. By combining the laser and plasmon resonance shift towards longer wavelengths we have achieved a great reduction in background fluorescence of blood. Great enhancement of Raman signal coming solely from drugs was achieved without any prominent lines coming from the erythrocytes. We have applied chemometric processing methods, such as Principal Component Analysis (PCA) to detect the elusive differences in the Raman bands which are specific for the investigated drugs. We have achieved good classification for the samples containing particular drugs (e.g., Butalbital, Pseudoephedrine). Furthermore, a quantitative analysis was carried out to assess the limit of detection (LOD) and limit of quantification (LOQ) using Partial Least Squares (PLS) regression method. In conclusion, our LOD and LOQ values obtained for each class of drugs was competitive with the gold standard GC/MS method.

[1] S. Siddhanta et al., Integration of protein tethering in a rapid and label-free SERS screening platform for drugs of abuse, Chemical Communications 52(58), 9016–9019 (2016).

[2] J. Smulko et al., Noise sources in Raman spectroscopy of biological objects, Proc. SPIE 10063, 100630Q (2017)

Towards Immunosensor for the Determination of GVA-Antigen Based on Photoluminescence of ZnO Films

A. Tereshchenko¹, V. Fedorenko^{1,2}, V. Smytyna¹, I. Konup³, A. Konup⁴, M. Eriksson⁵, R. Yakimova⁵, S. Balme², M. Bechelany², A. Ramanavicius⁶

¹ Experimental Physics Department, Odessa National I. I. Mechnikov University, Odessa, Ukraine.

² Institut Européen des Membranes IEMM, ENSCM UM CNRS UMR5635, Montpellier, France.

³ Department of Microbiology, Virology and Biotechnology, Odessa National I. I. Mechnikov University, Odessa, Ukraine.

⁴ National Scientific Centre "Institute of Viticulture and Wine Making Named After V. Ye. Tairov", Odessa, Ukraine.

⁵ Department of Physics, Chemistry and Biology, Linköping University, Linköping, Sweden.

⁶ Department of Physical Chemistry, Vilnius University, Vilnius, Lithuania

E-mail: alla_teresc@onu.edu.ua

Photoluminescence based immunosensor for the determination of Grapevine virus A-type (GVA) proteins (GVA-antigens) has been developed [1]. The immunosensor is based on ZnO thin films (100 nm thickness) formed on the Silicon substrates by atomic layer deposition. The ZnO-based films have demonstrated favorable surface-structural properties for the direct immobilization of antibodies against GVA-antigens in order to form a biosensitive layer sensitive to GVA antigens. The absorption of anti-GVA antibodies resulted in a new photoluminescence band appearance in the region of 400-550 nm that can be caused by the formation of some chemical bounds during the anti-GVA adsorption on ZnO surface. The possibility to detect GVA-antigens without additional labels (e.g enzymes or fluorescent dyes) has been demonstrated. The GVA-antigen detection was performed by the evaluation of changes and behavior of the photoluminescence band, related to protein adsorption (Fig. 1). The sensitivity of as-formed label-free biosensor towards the GVA-antigens was determined in the range from 1 pg/ml to 10 ng/ml.

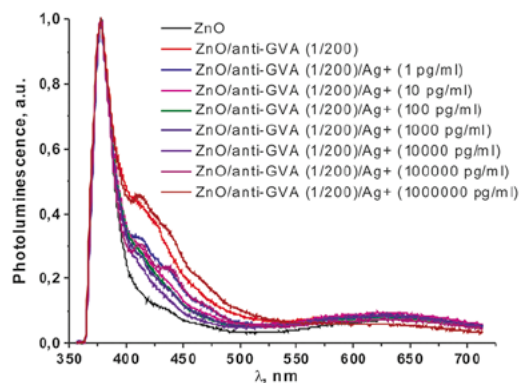


Fig. 1. Photoluminescence spectra of ZnO100nm/anti-GVA-based immunosensor under different GVA-antigen concentrations

Optical Investigation of Nanodiamonds Interactions with Blood

K. Karpienko¹, M. Wąsowicz², M. Ficek¹, M. Jędrzejewska-Szczerska¹

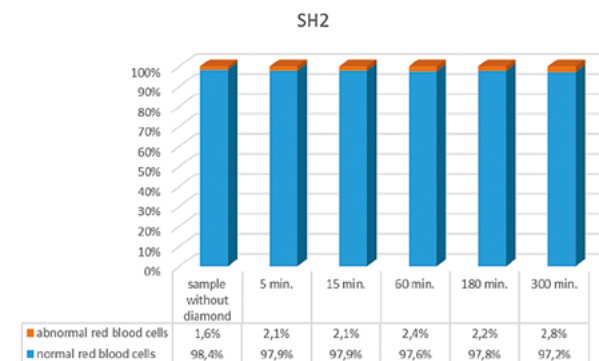
¹ Department of Metrology and Optoelectronics, Faculty of Electronics, Telecommunications and Informatics, Gdańsk University of Technology, Gdańsk, Poland

² Warsaw University of Life Sciences, Warsaw, Poland

E-mail: mateuszficek@gmail.com

The blood is complex bodily fluid containing plasma with various types of cells, including erythrocytes, leukocytes and platelets. In this study an interactions of nanodiamond particles with blood elements over various periods of time was investigated. Blood samples were taken from healthy dogs (Canis lupus f. domestica) of various age, different blood types and both sexes. During experiment, hydrogenated nanodiamonds (SH2) in two concentrations (20 μl and 100 μl suspended in saline) were added to blood samples. Then, samples were examined on microscopic images, and compared to blood samples without nanodiamonds. Number of normal and abnormal cells was marked for every 100 erythrocytes in both types of samples.

Results indicate that 20 μl concentration of hydrogenated nanodiamonds in the blood does not affect erythrocytes. Number of abnormal erythrocytes in samples with added SH2 is within the tolerable laboratory error.



Percentage of normal and abnormal erythrocytes (red blood cells) in prepared samples

[1] A. Tereshchenko et. al., ZnO films formed by atomic layer deposition as an optical biosensor platform for the detection of Grapevine virus A-type proteins, Biosensors and Bioelectronics, 92, 763–769 (2017)

PPG of Young and Elderly People, Clinical Patients, and Cohorts

M. Huotari¹, K. Määttä², J. Röning¹

University of OULU, ¹BISG, ²CAS, Oulu, Finland

E-mail: matti.huotari@ee.oulu.fi

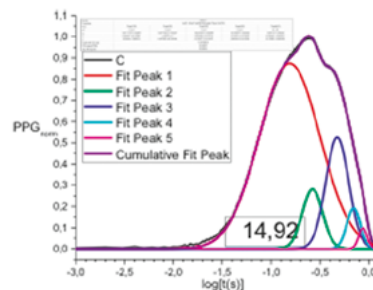
Biophotonic measurement devices could overcome the burden of healthcare units. Quantifying and monitoring health is becoming a great business interest. Innovative companies have been focusing on developing health technologies based on light, especially on photonic sensor technology, which enables non-invasive measurement of pulse waveforms.

Photoplethysmography (PPG) and signal analysis have many deep challenges. PPG pulse amplitude is either increasing or decreasing. Especially decreased amplitude (smaller pulses) are caused by vasoconstriction pharmacologically, physiologically (by cold, surgical-induced stress, increased tissue congestion (venous), hand or toe position lower than the heart. Increased PPG amplitude (larger pulses) are caused by vasodilation pharmacologically, physiologically (by warming, sedation, sepsis), or by regional blocks, decreased tissue congestion (venous), and hand or toe position held above the heart (when measured at the finger or toe). PPG provides a comfortable solution, as it does not require electrodes.

We calculate numerically the second derivative of PPG signals as measured in red and infrared light from finger, and toe. The responses we decompose for elasticity index (EI), Figure. The PPG signal is composed of the heart beat causing the percussion wave, followed by the tidal wave generated by the aorta. The other reflected waves are coming from the periphery as follows; dicrotic wave, reperfusion wave, and retidal wave based on the decomposition processing. However, the origins of the decomposed waveforms are not fully understood, it is generally accepted that PPG can provide clinical information on the cardiovascular system. The decomposed nonlinear curve fit gives COD over 0.999 ($=R^2$), and EI is 14.92. The nonlinear fitted curves were calculated for all study subjects.

The closed form solution for the arterial pulse waveform, e.g., PPG wave can be obtained from the fluid dynamic equations, but due to the intrinsic variability of parameters of the equations means that a closed form solution is impossible [1]. In nature, arterial wall properties change the arterial pulse waveform because of geometrical and wall tensional changes, which are impossible to measure but only by photonic means, e.g., by PPG [2].

By Origin software we can obtain the upper, lower, or both envelopes of the PPG data. Arterial EI then can be exactly determined as the arterial stiffness indicator.



A normalized decomposed PPG pulse (black) with its percussion (red), tidal (green), dicrotic (blue), reperfusion (cyan), and retidal (magenta) wave on logarithmic time axis. Envelope is violet.

[1] Erbay, HA, et al. (1987) Pulse waves in prestressed arteries. Bull.Math.Biol., 49:289-305.

[2] Demiray, H., Dost, S. (1990). Pulse waves in a prestressed elastic tube. International journal of engineering science, 28(1), 1-9.

Evaluation of Nitroglycerin Effect on Remote Photoplethysmogram Waveform

Z. Marcinkevics¹, U. Rubins², A. Caica¹, E. Dislere¹, A. Grabovskis²

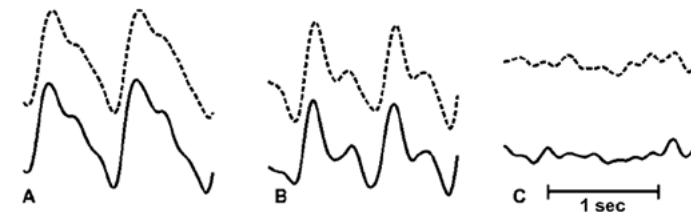
¹Department of Human and Animal Physiology, University of Latvia, Riga, Latvia

²Institute of Atomic Physics and Spectroscopy, University of Latvia, Riga, Latvia

E-mail: zbigis@latnet.lv

Assessment of skin microcirculation provides diagnostically valuable information at the early stages of pathologies, such as sepsis, diabetes and Reynold syndrome [1] and several optical techniques are available for evaluation. The simple and cost-effective alternative to existing methods is remote photoplethysmography (rPPG), with its ability to non-intrusively acquire signals at different cutaneous circulatory layers [2]. Traditionally robust parameters such as heart rate and perfusion index are extracted from rPPG signal, as analyses of waveform parameters in low intensity signal is still challenging. Therefore an important question is usefulness of rPPG signal waveform for diagnostic purpose.

Twelve healthy volunteers (age: 20-60 y.) gave informed consent and were enrolled in the study. The alterations of cardiovascular system (decrease of arterial stiffness) were induced by a single dose (1mg) sublingual administration of nitro-glycerine (NTG). The protocol comprised 3 minutes of baseline recording, 15 minutes recording of NTG effect, 2 minutes of arterial occlusion and the following 3 min reactive hyperaemia. Two PPG signals were acquired from glabrous skin of the middle finger distal phalange, consecutively at 560 nm and 810nm, 125 fps per channel, and systemic cardiovascular parameters were continuously registered in a beat-to-beat manner with a Finameter-midi system.



rPPG waveforms (530nm – dotted line; 810nm – solid line) at the baseline (A), during NTG administration and arterial occlusion (C).

The NTG effect was observed 0.7 - 1.2 minutes post administration, reaching maximum after 3 minutes. Systemic cardiovascular parameters significantly changed: systolic arterial pressure decreased for 9%, diastolic for 7%, mean arterial pressure for 5%, stroke volume for 20% and cardiac output for 12%, whereas the heart rate increased for 20%. Substantial alterations were observed for rPPG waveforms during NTG effect (see figure). DC component at 530nm decreased for 5% while at 810nm didn't change. The relative amplitude of diastolic peak decreased for 50% in both rPPG signals, indicating remarkable decrease of arterial stiffness and lower velocity of reflected wave propagation. During arterial occlusion rPPG waveforms disappeared, displaying noise (see, fig.C). It has been concluded that rPPG waveform may provide information related to arterial stiffness, and could be potentially utilised in the clinics.

[1] E.S. Nilsson, et al., "Non-invasive imaging of microcirculation: a technology review," Physiol. Med. Devices (Auckl), 7, 445-452, (2014).

[2] Z. Marcinkevics, et al., "Imaging photoplethysmography for clinical assessment of cutaneous microcirculation at two different depths," J. Biomed. Opt. 21(3), 35005 (2016).

Monitoring Soft Tissue Coagulation by Optical Spectroscopy

A. Lihachev¹, I. Lihacova¹, J. Spigulis¹, T. Trebst², M. Wehner³

¹Biophotonics lab., Institute of Atomic Physics and Spectroscopy, University of Latvia, Riga, Latvia

²LifePhotonic GmbH, Bonn, Germany

³Fraunhofer-Institut für Lasertechnik – ILT, Aachen, Germany

E-mail: martin.wehner@ilt.fraunhofer.de

Laser tissue welding (LTW) or laser tissue soldering (LTS) is investigated since many years for treatment of incisions, wound closure and anastomosis of vessels [1, 2]. Depending on the process, a certain temperature in the range between 65 °C to 85 °C must be reached and held for a few seconds. Care has to be taken not to overheat the tissue; otherwise necrosis or tissue carbonization may occur and will impair wound healing. Usually the temperature is monitored during the process to control the laser power [3]. This requires either bulky equipment or expensive and fragile infrared fibres to feed the temperature signal to an infrared detector. Alternatively, changes in tissue morphology can be directly observed by analysis of spectral reflectance. The reduced scattering and absorption coefficients were deduced from spectra by inverse Monte-Carlo model and averaged over 430 – 530 nm spectral range to get a significant signal for morphological tissue changes [4]. In our work we propose a simpler method by comparing the signal strength from different spectral bands to reveal the onset of tissue coagulation. Our measurements are in good correlation with the temperature increase of tissue samples. We conclude that simple spectroscopy in the visible range can provide valuable information during LTS and LTW and probably replace the delicate measurement of temperature. A major advantage is that optical measurements can be performed using standard optical fibres and can be easily integrated into a surgical tool.

[1] K.M.McNally-Heintzelman et al, "Laser Tissue Welding," in Biomedical Photonics Handbook, Florida, USA, CRC Press, , pp. 39-1 - 39-30. (2003).

[2] D.S. Scherr et al., "Laser tissue welding", Urol Clin North Am, 25, 123-135. (1998).

[3] O. Eyal et al, "Thermal feedback control techniques for transistor-transistor logic triggered CO₂ laser used for irradiation of biological tissue utilizing infrared fiber-optic radiometry", Appl Opt, 33, 1751-1754 (1994).

[4] V.K. Nagarajan et. al., "Monitoring of tissue optical properties during thermal coagulation of ex vivo tissues", Lasers Surg Med., 48(7), 686-94 (2016)

Study of Capsaicin-induced Changes of Blood Circulation by Imaging Plethysmography

M. Volynsky¹, R. Giniatullin^{1,2,3}, O. Mamontov^{1,4,5}, A. Kamshilin¹

¹ITMO University, Saint Petersburg, Russia

²Kazan Federal University, Kazan, Russia

³University of Eastern Finland, Kuopio, Finland

⁴Pavlov First Saint Petersburg State Medical University, Saint Petersburg, Russia

⁵Federal Almazov North-West Medical Research Centre, Saint Petersburg, Russia

E-mail: maxim.volynsky@gmail.com

Migraine is the most common neurological disorder with still little understood pathophysiology involving both somatic and autonomous nervous system along with disturbances in vascular reactivity. Therefore, it is important to develop valuable biomarkers of migraine in individual patients.

We recently reported the role of capsaicin activated TRPV1 receptors in migraine pathology [1]. Moreover, dermal blood flow changes to local application of capsaicin are commonly used to evaluate the efficacy of anti-migraine drugs [2]. However, this approach is based on simple vasodilation of skin vessels.

The aim of our study was to use our recently developed imaging photoplethysmography (IPPG) approach [3], to explore detailed characteristics of microcirculation in healthy subjects and migraine patients exposed to capsaicin patch.

Here we report our preliminary data obtained from several healthy volunteers. After obtaining baseline parameters of blood flow in the forearm, we applied the capsaicin patch for 60 min. The parameters of the blood flow were also recorded during application and after the removal of the capsaicin patch. We found that the amplitude of blood pulsations at the site of application and surrounding regions was significantly increased during the application and in 10-15 minutes returned to the initial values after removal. The rates of blood-pulsations-amplitude increase during the first stage and decrease during the second stage could serve as a parameter to characterize the reaction of local blood perfusion on capsaicin application.

In summary, we suggest a novel advanced approach for measurements of the reactivity of local blood flow in response to capsaicin by using the method IPPG which can be applied for the objective diagnosis of migraine and for selection of effective antimigraine therapy.

ACKNOWLEDGEMENTS

The work was supported by the Russian Science Foundation (Grant No. 15-15-20012).

[1] A.Zakharov et al. Hunting for origins of migraine pain: cluster analysis of spontaneous and capsaicin-induced firing in meningeal trigeminal nerve fibers, Frontiers in Cellular Neuroscience, vol. 9, article 287, pp. 1-14 (2015).

[2] L.Shi et al. Pharmacologic Characterization of AMG 334, a Potent and Selective Human Monoclonal Antibody against the Calcitonin Gene-Related Peptide Receptor, Journal of Pharmacology and Experimental Therapeutics, vol. 356, No. 1, pp. 223-231 (2015).

[3] A.A.Kamshilin et al. Accurate measurement of the pulse wave delay with imaging photoplethysmography, Biomedical Optics Express, vol. 7, No. 12, pp. 5138-5147 (2016).

Color Constancy in Dermatoscopy with Smartphone

B. Cugmas, F. Pernuš, B. Likar

Laboratory of Imaging Technologies, Faculty of Electrical Engineering,
University of Ljubljana, Ljubljana, Slovenia

E-mail: blaz.cugmas@fe.uni-lj.si

The recent spread of cheaper smartphone dermatoscopes (the selling price is few hundred dollars) can have an important impact on dermatology since the dermatoscopy is becoming easily available to the general practitioners and also to the patients. The latter are now able to acquire skin images on their own and to send them to dermatologists. Since these images will be acquired by different smartphone cameras, the variability in colors is expected. Therefore, dermatoscope mobile systems should be calibrated in order to ensure the color constancy in skin images.

In this study, we have tested color constancy of a system with a dermatoscope DermLite DL1 basic, used on the Samsung Galaxy S4 smartphone. Under the controlled conditions, jpeg images of 24 ColorChecker patches were acquired and used for a model between an unknown device-dependent RGB and a device-independent Lab color space. The linear system was solved with singular value decomposition (SVD) method.

Results showed that median and the best color reproduction accuracy was 7.4 and 4.9, respectively. In the video and printing industry, color reproduction accuracy is expected to be between 5 and 6. Since the skin does not exhibit all the colors used from ColorChecker, we assume that color reproduction accuracy could be even better if the system was calibrated in more narrow color range. It can be concluded that a calibrated smartphone dermatoscope can provide sufficient color constancy and can serve as an interesting opportunity to bring dermatology closer to the patients.

Image Quality Enhancement for Skin Cancer Optical Diagnostics

D. Bliznuks¹, I. Kuzmina², K. Bolocko¹, A. Lihacovs²

¹Faculty of Computer Science and Information Technology, Riga Technical University, Riga, Latvia

²Biophotonics Laboratory, Institute of Atomic Physics and Spectroscopy,
University of Latvia, Riga, Latvia

E-mail: dmitrijs.bliznuks@rtu.lv

Biophotonic area as many others research fields strongly rely on obtained image quality. The quality of image is a combination of the capabilities of hardware (camera/image sensor), optical system and image post processing. A lot of biophotonic methods use reference sample and calibration in post processing. That allows reducing the effect of all imperfections. Nevertheless, some of the methods require images of sufficient quality before post processing. That happens when imaged object reacts in nonlinear and dynamical way and obtaining of a calibration function is not possible. Some of imaging sensors implement pre-processing when illumination is close to extreme zones (dark or bright), therefore it might bring errors to diagnostics, since diagnostic algorithms expect that intensity and image pixel values have linear relationship.

We focus on two specific methods that are used for skin cancer optical diagnostics: fluorescence photo-bleaching and diffuse reflectance. Experiments of photobleaching [1] require high level of homogeneity of ultraviolet illumination source, since skin reacts in nonlinear and dynamical way to illumination intensity. Since obtained image includes all optical system's imperfections, there is a task to separate optical imperfections that could be compensated from light source illumination non-uniformity that is hardly correctable. Along with homogeneity issue, photo-bleaching demands stable illumination intensity all over the experiment time. Since experiment might last up to 20s [2], light emitting diodes heat up and change their intensity. The paper proposes several techniques for minimizing intensity changes, including thermal controlling, intensity correction with and without feedback loop. Diffuse reflectance algorithms have less strict requirements, nevertheless the problem of getting in the extreme zones remains.

Our research includes techniques for separating image imperfection sources among optics, illumination and imaging sensor. We propose methods for parametrizing of image sensor to obtain maximal quality and checking if the region of interest is in the extreme zones (bright or dark). We propose the set of experiments that will allow to evaluate imaging system and to get the optics' calibration function. The calibration function includes illumination non-uniformity/instability, optics imperfections (e.g. lens vignetting), thermal noise, gain noise, and intensity curve nonlinearity. All above mentioned image enhancement techniques can improve the quality of disease detection for skin cancer diagnostics as well as for other applications, where image post processing is limited.

ACKNOWLEDGEMENTS

This work has been supported by European Regional Development Fund project "Portable Device for Non-contact Early Diagnostics of Skin Cancer" under grant agreement # 1.1.1.1/16/A/197.

[1] A. Lihachev et al., "Autofluorescence imaging of basal cell carcinoma by smartphone RGB camera", J. Biomed. Opt. 20(12), 120502 (2015).

[2] J. Spigulis et al., "Imaging of laser-excited tissue autofluorescence bleaching rates," Appl. Opt. 48, D163-D168, (2009)

Computer Simulation of Skin Dermoscopy Images

M. Iralieva, O. Myakinin, I. Bratchenko, V. Zakharov

Laser and Biotechnical Systems Dept., Samara University, Samara, Russia

E-mail: malica.iralieva@gmail.com

The computer dermoscopy is a key tool for the quick and noninvasive skin cancer diagnostics [1]. Large amount of skin cancer images requires to verify malignant neoplasm recognition algorithm. Sometimes, it is impossible to collect so many images for statistically proved results. The main purpose of this work is to create a program tool for modeling of various skin cancer tumor images.

A self-made dermoscopy imaging tool is shown on Fig.1 (a). The tool has 2 polarized white LEDs (39lm, 4000K), 2 unpolarized white LEDs (39lm, 4000K), 1 blue LED (30lm, 465-485 nm), 1 green LED (52lm, 520-535 nm), 1 red LED (46lm, 620-6305 nm) and a camera (RGB, 12 bit/Pix, 1920*1080, ~13microns/Pix on skin surface). An example of a dermoscopy image is shown on Fig.1 (b). One of the most well-known methods to generate realistically structures is Fractal Perlin noise [2]. The Fractal Perlin noise has been added to Gauss function to simulate a cancer texture in the foreground. Normal background skin has been simulated by mixed Monte Carlo method [3] using a special online tool <http://biophotonics.fi/>.

Features of malignant skin tumors have been discussed; also as an algorithm of mathematical modeling for graphical representation of skin cancer is proposed. A program code to generate images of skin cancer for MATLAB R2014 has been developed. Graphical representation of the different dermoscopic structures is obtained (Fig.1(c)).

The proposed algorithm may be used to create a wide database of images with well-known and unusual rare cancer texture features for the dermoscopy imaging tool.

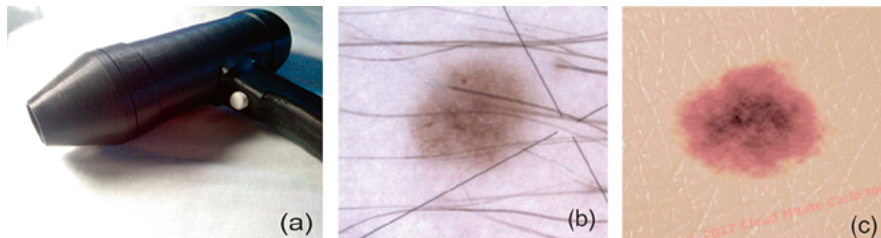


Fig. 1. Dermoscopy imaging tool (a), a dermoscopy image (b), an example of simulated dermoscopy image (c)

Keywords: skin cancer modeling, skin cancer tumor, Fractal Perlin noise, dermoscopy, dermoscopy imaging.

ACKNOWLEDGEMENTS

This research was supported by the Ministry of Education and Science of the Russian Federation.

Semi-automated Non-invasive Diagnostics Method for Melanoma Differentiation from Nevi and Basal Cell Carcinomas

I. Lihacova¹, K. Bolocko², A. Lihachev¹

¹Institute of Atomic Physics and Spectroscopy, University of Latvia, Riga, Latvia

² Faculty of Computer Science and Information Technology, Riga Technical University, Riga, Latvia

E-mail: ilze.lihacova@lu.lv

The incidence of skin cancer is still increasing not only in Latvia but also in other parts of Europe [1]. Late tumor detection is the main reason of the high mortality associated with skin cancer. The accessibility of early diagnostics of skin cancer in Latvia is limited by several factors, such as high cost of dermatology services, long queues on state funded oncologist examinations, as well as inaccessibility of oncologists in the countryside regions – this is an actual clinical problem. The new strategies and guidelines for skin cancer early detection and post-surgical follow-up intend to realize the full body examination (FBE) by primary care physicians (general practitioners, interns) in combination with classical dermoscopy [2]. To implement this approach, a semi-automated method was established. Newly developed software analyzes 3 multispectral images of skin malformation at different wavelengths [3, 4]. First results show that it is possible to perform automatic image analysis by excluding a number of artifacts – skin hair, movement, skin curvature, direct reflection and get reliable melanoma differentiation from nevi and basal cell carcinomas.

ACKNOWLEDGEMENTS

This work has been supported by European Regional Development Fund project "Portable Device for Non-contact Early Diagnostics of Skin Cancer" under grant agreement # 1.1.1.1/16/A/197.

[1] J.Ferlay et al., "Cancer incidence and mortality patterns in Europe: Estimates for 40 countries in 2012," EUR J CANCER 49(6), 1374-1403 (2013).

[2] R.Shellenberger et al., "Melanoma screening: A plan for improving early detection," Ann Med. 48(3), 142-8, (2016).

[3] U.Rubins et al., "Multispectral video-microscope modified for skin diagnostics," Latv. J. Phys. Tech. Sci, 51(5), 65-70 (2014).

[4] I.Diebele et al., "Clinical evaluation of melanomas and common nevi by spectral imaging," Biomed. Opt. Express 3(3), 467-472 (2012).

Development of Optical WGM Resonators for Biosensors

I. Brice, A. Pirkina, A. Ubele, K. Grundsteins, A. Atvars, R. Viter, J. Alnis

Institute of Atomic Physics and Spectroscopy, University of Latvia, Riga, Latvia

E-mail: janis.alnis@lu.lv

Optical whispering gallery mode (WGM) resonators are made of a round-shaped optically transparent material and keep a circulating light wave inside using the effect of total internal reflection. WGM resonators allow to significantly increase the effective light path length allowing sensitive detection of molecules attaching to the surface [1]. Other advantages are suitability for a wide range of optical radiation, compactness, simplicity and low cost.

To obtain the sensitivity of WGM resonators on certain biomolecules, they have to be covered with special nanolayers (ZnO, TiO₂), nanoparticles (Au) and polymers (PANI, Ppy)). A biofunctionalization of the metal oxide surface will be performed with (3-Aminopropyltriethoxysilane (APTES). After biofunctionalization, the antigens/antibodies will be deposited on the nanostructured surfaces of WGM to form bioselective layers.

The tests will be carried to test the sensitivity of these WGMR to various biomolecules. For this absorption and fluorescence spectra will be obtained. Structure properties of the novel WGM materials will be studied with Scanning electron microscopy, Atomic force microscopy and X-ray diffraction. The sensitivity of the modified WGM biosensors will be studied in the range of pg/ml-ng/ml concentrations of the target molecules. Response time and adsorption constants will be calculated from kinetic measurements.

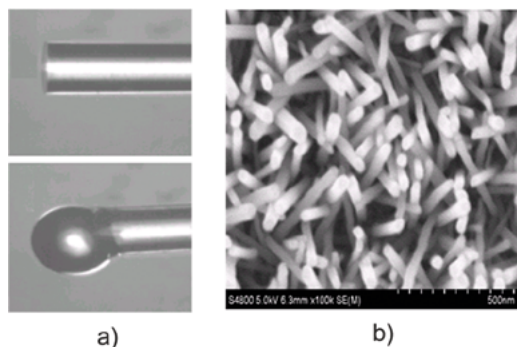


Fig. 1. a) WGM resonator produced by melting a tip of an optical fiber in a flame; b) SEM image of ZnO nanorod layer on the WGM resonator surface.

ACKNOWLEDGEMENTS

We thank for support ERAF project Nr.1.1.1.1/16/A/259: "Development of novel WGM microresonators for optical frequency standards and biosensors, and their characterization with a femtosecond optical frequency comb".

Water Content in Human Liver from Dispersion Evaluation

I. Carneiro¹, S. Carvalho¹, R. Henrique^{1,2}, L. Oliveira^{3,4}, V. Tuchin^{5,6,7}

¹ Portuguese Oncology Institute of Porto – Department of Pathology and Cancer Biology and Epigenetics Group-Research Centre, Porto, Portugal

² Institute of Biomedical Sciences Abel Salazar (Porto University) – Department of Pathology and Molecular Immunology, Porto, Portugal

³ Engineering School of Polytechnic of Porto – Physics Department, Porto, Portugal

⁴ Centre of Innovation in engineering and Industrial Technology, Porto, Portugal

⁵ Research-Educational Institute of Optics and Biophotonics – Saratov National Research State University, Saratov, Russia

⁶ Laboratory of Laser Diagnostics of Technical and Living Systems – Precision Mechanics and Control Institute of the Russian Academy of Sciences, Saratov, Russia

⁷ Interdisciplinary Laboratory of Biophotonics – National Research Tomsk State University, Tomsk, Russia

E-mail: lmo@isep.ipp.pt

Biological tissues have internal heterogeneous composition. Generally, tissues are composed by solid components, which are permeated by interstitial fluids. The purpose of interstitial fluids is to provide hydration to the solid components and to contain some dissolved salts and organic compounds, which are necessary for physiological processes [1].

The interstitial fluids are mainly composed by water, which has a low refractive index, relative to the refractive index of the solid components. Such difference in the refractive index of tissue components is responsible for strong light scattering inside the biological tissues [1]. When optical clearing treatments are to be prepared, it is necessary to know the amount of water inside a tissue, so the correct concentration of the optical clearing agent is selected.

The global refractive index of a tissue is a weighted combination of the partial contributions from the refractive indices of the tissue components. Considering a tissue model that considers only water and solid components, the Beer-Lambert equation can be used to estimate the water content in the tissue [2].

Measuring the refractive index of human liver tissues using the total internal reflection method at various laser wavelengths [3], we have estimated the corresponding dispersion curve. Considering the above simplified model for the liver, we have calculated the water content and the dispersion for the solid liver components as a whole by subtracting the water contribution in the liver dispersion curve. The calculated dispersion for the solid components can be later used to calculate the time dependence of the liver dispersion curve during optical clearing treatments, provided that thickness and collimated transmittance measurements are made during the treatments [4].

[1] Tuchin, Optical Clearing of Tissues and Blood, SPIE Press, 2-3 (2006).

[2] Oliveira et. al., Diffusion characteristics of ethylene glycol in skeletal muscle, Journal of biomedical Optics, 051019-1-10 (2015).

[3] Carvalho et. al., Wavelength dependence of the refractive index of human colorectal tissues: comparison between healthy mucosa and cancer, Journal of Biomedical Photonics & Engineering, 040307-1-9 (2016).

[4] Oliveira et. al., Skeletal muscle dispersion (400 – 1000 nm) and kinetics at optical clearing, Journal of Biophotonics, Submitted

[1] F.Vollmer et al., Whispering-gallery-mode biosensing, Nature Methods 5, 591 (2008)

Toxoplasmosis Diagnostics Based on Photoluminescence of Zinc Oxide Nanoparticles

M. Galat, N. Shpyrka, M. Taran, O. Pareniuk, K. Shavanova, O. Boiko

National University of Life and Environmental Sciences of Ukraine, Kyiv, Ukraine

E-mail: galat_mv@nubip.edu.ua

Toxoplasma gondii is a common agent of protozoan disease of different kinds of animals and humans. That is why timely and accurate diagnosis of the disease is important. That is why a new method for the diagnosis of toxoplasmosis based on photoluminescence of nanoparticles of zinc oxide was developed and tested. Photoluminescence spectra of *Toxoplasma* biomolecules on the surface of ZnO were recorded through fiber-optic spectrometer, and the method of scanning electron microscopy was used to study the nanorods microstructure.

As a result of studies it was revealed that immune complexes biosensor based on zinc oxide have sufficient specificity reaction taking into account the significant reduction of signal when making specific serums with the dilution of 1:5. Reduction of the photoluminescence intensity indicates the formation of nanorods biocomplexes on the surface of zinc oxide on a "key-lock" principle which is accompanied by a modification of the pre-adsorbed antibody molecules structure.

Based on the obtained results, it is possible to state that described method has high detection rate and relatively low complexity of the application. Further study and improvement of methods of diagnosis of toxoplasmosis using immune biosensor will enable cheaper diagnosis of the disease process and accelerate it.

Speckle Scattering Studies from Red Blood Cell Suspension

David Joseph

Physics department, Guru Jambheshwar University of Science and Technology, Hisar, India

E-mail: davidjp07@gmail.com

Spectacular scattering from rough surfaces give information about the morphology as well as the texture of surfaces. This reveals the physical quantities like Mean, Histogram, Kurtosis and skewness properties of the rough surfaces [1]. The present study is an attempt to model the Red blood cells (RBC) as rough scatterers illuminated by laser light. The transmitted light has three components: the transmitted intensity, scattered intensity and the fluctuations due to Brownian motion. The scattered part has the scattering properties described by Mie scatterers and also the morphological part revealed by the speckle scattering from surfaces. The convolution of these components in scattering is a mathematical problem [2-3]. The time evolution of the roughness parameters are also studied in this work.

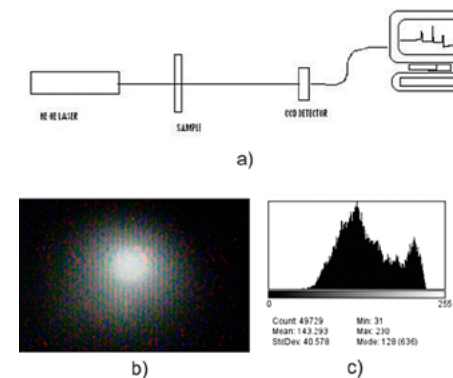


Fig. 1. Speckle set up used for red Blood cells (a), typical Speckle pattern (b) and the histogram (c).

The experiential set up consists of the He-Ne laser, Cuvette mounted on a spectrometer Turn Table and the CCD detector interfaced with a computer. The ImageJ software computes the roughness parameters: Mean, Histogram, Kurtosis and skewness. Typical speckle pattern and the corresponding Histogram are shown in Fig.1 (b, c).

RESULTS AND CONCLUSION

This study has been done in the forward scattering angle. However this study can be extended to other scattering angles which can give very spectacular speckle scattering properties. Scattering particles being in constant Brownian motion due to thermal energy can have a negative effect. However, the ensemble average of these fluctuations may be averaged out in sensitive data collection.

[1] K. Y. Ahn et al., A sensitive diagnostic assay of rheumatoid arthritis using three-dimensional ZnO nanorod structure// Biosensors & Bioelectronics, 28 (1), 378–385 (2011).

[2] J.P.Dubey et al., Toxoplasma gondii infection in humans and animals in the United States. Internal Journal of Parasitology, 38, 1257–1278 (2008)

[3] R.Viter et al., Application of Room Temperature Photoluminescence From ZnO Nano-rods for Salmonella Detection, IEEE Sensors Journal, 14(6), 2028–2034 (2014).

[1] K. Creath et al., "Absolute Measurement of Surface Roughness", Applied optics 29, p.3823-3827 (1990).

[2] BeckmannP & Spizzichino A, "The Scattering of Electro-Magnetic Wave from Rough Surface", Pergamon, New York (1963).

[3] M. Shiraishi et al., "Possibility of Large Roughness Measurement by Laser Speckle", Transaction of the ASME, 113, p.476 (1991)

Application of Quantum Dots CdZnSeS/ZnS Luminescence, Enhanced by Plasmons of Roughness Silver Surface for Detection of Albumin in Blood Facies of Infected Person

**E. Konstantinova^{1,2}, A. Zyubin², V. Slezhkin^{1,2}, E. Moiseeva²,
K. Matveeva², V. Bryukhanov²**

¹ Kaliningrad State Technical University, Kaliningrad, Russia

² Immanuel Kant Baltic Federal University, Kaliningrad, Russia

E-mail: konstantinovaeliz@gmail.com

It is known that the detection, for example, of proteins and salts in biological fluids plays an important role in the clinical diagnosis [1]. Modern nanomaterials (metallic nanoparticles, quantum dots, fullerenes and so on.) used for the analysis of biological tissue can increase the sensitivity of optical methods, which makes possible their application both at the early stage of the disease diagnosis, and when monitoring the of therapeutic treatment dynamics [2].

In the present work, the human albumin samples allotted from the blood plasma of a healthy person and infected, with the manifestation of sepsis, have been studied. The protein film (facies) obtained by the method of a wedge-shaped drop dehydration of the albumin solution at the concentration of $C=1 \times 10^{-5} \text{ M}$ on the rough silver surface with quantum dots CdZnSeS/ZnS (QDs) as a fluorescent marker by spectral-kinetic methods has been studied.

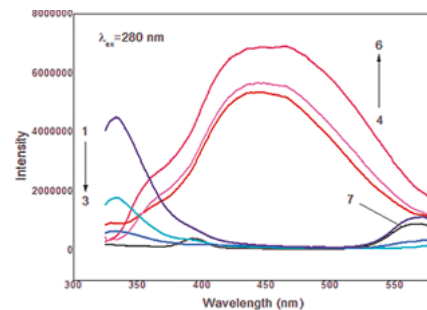


Fig. 1. The luminescence spectra of healthy human albumin (1 - 3) and infected with manifestation of sepsis (4 - 6) on rough silver surface with CdZnSeS/ZnS (7) quantum dots of different concentrations: 1, 4, 7 - $N=1 \cdot 10^{12} \text{ cm}^{-2}$, 2, 5 - $N=2 \cdot 10^{12} \text{ cm}^{-2}$, 3, 6 - $N=3 \cdot 10^{12} \text{ cm}^{-2}$.

In the study of facies on a rough silver surface with the QDs the shift of the fluorescence spectrum maximum to the long-wave region (Fig. 1) has been found, which indicates the interaction of the protein and QD. In addition, the luminescence intensity of quantum dots with the protein increases, which also confirms their interaction. Nonradiative electron energy transfer from the protein to the QDs with an increase in the QDs concentration in the case of a healthy protein is observed [3]. The luminescence intensity of QDs increases in the presence of the infected protein, and a broad band appears with a maximum at 450 nm, which is apparently due to the formation of complexes from aggregated residues of various proteins and salts.

[1] Powers A. D. et al., Protein analytical assays for diagnosing, monitoring, and choosing treatment for cancer patients, Journal of healthcare engineering, vol. 3, pp. 503–534 (2012).

[2] Baetke S. C. et al., Applications of nanoparticles for diagnosis and therapy of cancer, The British journal of radiology, vol. 88, pp. 20150207 (2015).

[3] Xiao Q. et al., Conformation, thermodynamics and stoichiometry of HAS adsorbed to colloidal CdSe/ZnS quantum dots, Biochimica et Biophysica Acta, vol. 1784, pp. 1020–1027 (2008)

Towards In Vivo Skin Cancer Detection by Colour Parameters

I. Kuzmina¹, E. Borisova², Ts. Genova², P. Troyanova³, J. Spigulis¹

¹ Biophotonics Lab., Institute of Atomic Physics and Spectroscopy, University of Latvia, Riga, Latvia

² Biophotonics Lab., Institute of Electronics, Bulgarian Academy of Sciences, Sofia, Bulgaria

³ University Hospital "Tzaritza Yoanna-ISUL", Sofia, Bulgaria

E-mail: ilona.kuzmina@lu.lv

Diffuse reflectance and colour parameters of different skin lesions have been studied previously for non-invasive diagnostics [1, 2]. Diffuse reflectance spectroscopy has been recognized as a good tool for pigmented skin lesions' differentiation [1]. $L^*a^*b^*$ colour parameters showed promising results for a therapy monitoring of skin vascular lesions [2].

In this research we performed in vivo diffuse reflectance measurements on different lesions such as seborrheic keratosis, dermal and dysplastic nevi, basal cell carcinoma (BCC), squamous cell carcinoma (SCC) and melanoma in the University Hospital "Tzaritsa Yoanna-ISUL". Seborrheic keratosis and dermal nevi are considered benign skin malformations, while BCC, SCC and melanoma are malignant lesions, dysplastic nevi are specific moles which have a tendency to transform into melanoma more often than ordinary ones.

The measurements were made using tungsten halogen as a light source, USB4000 spectrometer (Ocean Optics Inc.), and a fibre optic cable of 7 fibres: one was used for illumination, the other six – for signal detection. Acquired reflectance spectra of the lesion and healthy skin were used for calculation of CIE xyY and $L^*a^*b^*$ colour parameters.

The results showed that colour parameters can be used for skin lesions diagnostic however larger lesions' groups have to be analysed for convincing conclusions.

ACKNOWLEDGEMENTS

This work has been supported by COST action BM1205 "European network for skin cancer detection using laser imaging".

[1] E. Borisova et al "Optical Biopsy of Human Skin – A Tool for Cutaneous Tumours' Diagnosis" Int. J. Bioautomation, 16(1), 53-72 (2012).

[2] I. Kuzmina et al "Contact and contactless diffuse reflectance spectroscopy: potential for recovery monitoring of vascular lesions after intense pulsed light treatment" J. Biomed. Opt., 16(4), 040505-1-3 (2011)

Rosacea Assessment by Erythema Index and Principal Component Analysis Segmentation Maps

I. Kuzmina, U. Rubins, I. Saknite, J. Spigulis

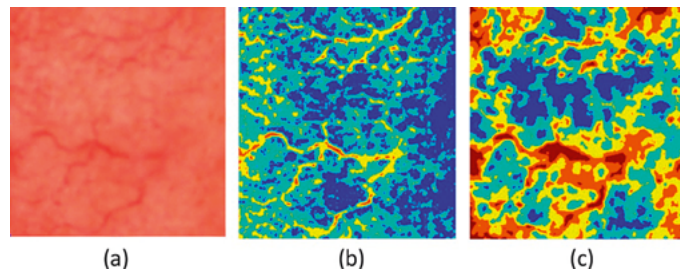
Biophotonics Laboratory, Institute of Atomic Physics and Spectroscopy, University of Latvia, Riga, Latvia

E-mail: ilona.kuzmina@lu.lv

Rosacea is a chronic inflammatory facial skin disease that involves erythema and visible blood vessels. Dermatologists evaluate severity of rosacea visually using Clinician's Erythema Assessment (CEA) grading scale [1]. There are also spectroscopic devices (e.g. Mexameter®) for erythema assessment, but mostly these devices estimate a small region of skin using a single photodetector.

In this research we used RGB images of rosacea lesions that were acquired by Sklmager (imaging prototype developed in the Institute of Atomic Physics and Spectroscopy [2]) in the previous study [3]. The images were used for calculation and segmentation of erythema index (EI) and principal component analysis (PCA) maps. In this study only the first three components of PCA were estimated. The erythema index was calculated by dividing red with green images. Segmentation was made by Otsu's method. The areas of the segmented regions were analysed and compared.

Results show that EI and PCA first component maps can be used for area estimation of visible blood vessels. An example of RGB image and segmented maps of a rosacea lesion is shown in the picture. The algorithm used in this study segments EI maps more precisely than the maps of the PCA first component. The PCA maps are also more influenced by shadows that appear in the images of curved face regions, and the algorithm doesn't distinguish blood vessels from shadows and pigmentation in these maps.



RGB image (a) and segmented maps of erythema index (b) and PCA (c) of a rosacea lesion

ACKNOWLEDGEMENTS

This work has been supported by Latvian National Research Programme "Cyber-physical systems, ontologies and biophotonics for safe and smart city and society" (SOPHIS) under grant agreement #10-4/VPP-4/11.

[1] J. Tan et al. "Reliability of Clinician Erythema Assessment grading scale", J. Am. Acad. Dermatol., 71, 760–763 (2014).

[2] J. Spigulis et al. "Sklmager: a concept device for in-vivo skin assessment by multimodal imaging", Proc. Est. Acad. Sci., 63 (3) 301–308 (2014).

[3] I. Saknite et al. "Comparison of single-spot technique and RGB imaging for erythema index estimation", Physiol. Meas., 37, 333–346 (2016)

Refractometry and Fluorescence Spectroscopy of Hemoglobin from Whole Blood of Rats with Alloxan Diabetes

E. N. Lazareva^{1,2,3}, P. A. Timoshina^{1,2}, D. K. Tuchina^{1,2}, V. I. Kochubey^{1,2}, A. B. Bucharskaya⁴, D. A. Alexandrov⁴, I. G. Samusev⁵, N. A. Myslitskaya^{5,6}, V. V. Bryukhanov⁵, V. V. Tuchin^{1,2,7}

¹ Research Educational Institute of Optics & Biophotonics, Saratov National Research State University, Saratov, Russia

² Interdisciplinary Laboratory of Biophotonics, National Research Tomsk State University

³ Center for Functionalized Magnetic Materials (FunMagMa), Immanuel Kant Baltic Federal University, Kaliningrad, Russia

⁴ Saratov State Medical University, Russia

⁵ Immanuel Kant Baltic Federal University, Kaliningrad, Russia

⁶ Kaliningrad State Technical University, Kaliningrad, Russia

⁷ Laboratory of Laser Diagnostics of Technical and Living Systems, Institute of Precision Mechanics and Control RAS, Saratov, Russia

E-mail: LazarevaEN@list.ru

The structure and optical properties of biological tissue change with the development of pathology. The use of refractometry and fluorescence spectroscopy in medical diagnostics are the urgent technologies. Several research groups proposed to use the refractive index as a marker for the differentiation of normal and pathological biological tissue, including experimental diabetes in animals [1–3]. It was found recently that the shape of the fluorescence band at 320 nm-excitation indicates hyperglycemia [4].

This pilot study is focused on measurement of the refractive index and the fluorescence spectra of hemoglobin obtained by hemolysis of whole blood of rats with alloxan diabetes. The refractive index was measured using a multi-wavelength Abbe refractometer (Atago, Japan) at wavelengths of 480, 486, 546, 589, 644, 656, 680, 930, 1100, 1300 and 1550 nm for temperature range from 27 to 50°C. Fluorescence spectra were measured using Spectral modular fluorometer Fluorolog-3 (HORIBA, Japan). The excitation wavelength was 260, 270 and 280 nm. The analysis of refractive index and fluorescence spectra obtained from blood hemoglobin samples revealed that the major differences between the control group of rats and animals with hyperglycemia were observed for the temperature increment of the refractive index and for fluorescence at 260 nm-excitation. The results obtained can serve as a good basis for combined technology for discrimination of normal and hyperglycemic states.

[1] O. S. Zhernovaya, V. V. Tuchin, I. V. Meglinski, Monitoring of blood proteins glycation by refractive index and spectral measurements, Las. Phys. Lett., 5(6), 460–464 (2008).

[2] P. Giannios, S. Koutsoumpas, K.G. Toutouzas, M. Matiatou, G.C. Zografos, and K. Moutzouris, Complex refractive index of normal and malignant human colorectal tissue in the visible and near-infrared, J. Biophotonics 10(2), 303–310 (2017).

[3] S. Carvalho, N. Gueiral, E. Nogueira, R. Henrique, L. Oliveira, V. V. Tuchin, Wavelength dependence of the refractive index of human colorectal tissues: comparison between healthy mucosa and cancer, J of Biomedical Photonics & Eng. 2(4) 040307-9 (2016).

[4] E. Shirshin, O. Cherkasova, T. Tikhonova, E. Berlovskaya, A. Priezhev, V. Fadeev, Native fluorescence spectroscopy of blood plasma of rats with experimental diabetes: Identifying fingerprints of glucose-related metabolic pathways, Journal of Biomedical Optics 20, 051033-8 (2015)

Evaluation of Skin Pathologies by RGB Autofluorescence Imaging

A. Lihachev¹, E. V. Plorina¹, A. Derjabo², M. Lange¹, I. Lihacova¹

¹Biophotonics Lab., Institute of Atomic Physics and Spectroscopy, University of Latvia, Riga, Latvia

²Riga East University Hospital, Oncology Centre of Latvia, Riga, Latvia

E-mail: aleksejs.lihacovs@lu.lv

Autofluorescence images of healthy and diseased human skin under continuous 405 nm LEDs excitation at a power density of ~ 7 mW/cm² with a frame rate 0.5 fps were recorded by smartphone RGB camera and further analysed using Python and Matlab software [1]. Overall images from 61 subjects of healthy skin, benign and malignant lesions were investigated. In order to visualize the skin AF decrease rates during the continuous excitation, the following image processing expression were applied:

$I(t) = a \exp\left(-\frac{t}{\tau}\right) + A$ (1), where t is time, $I(t)$ – AF intensity in a given moment, A – residual intensity or background intensity, τ – time constant and a – fitting constant. Photobleaching parameters (A , τ and a) were calculated using non-linear least-square regression analysis. The planar distribution of fitting parameters was performed using Python software. The G channel of acquired RGB images where stacked by time taken into a 3D array. Non-linear least-square regression analysis was performed on each corresponding pixel in the stack. The output is a 2D array of fitting parameters (A , τ , a) in each stack of pixels. Quantification of the AF photobleaching parameters for each particular case was performed by calculation of mean values of the parameters in pathology area and surrounding healthy skin. To estimate the efficiency of the proposed analysis the mean values of the photobleaching parameters according to diagnosis were plotted in scatter chart (Fig. 1).

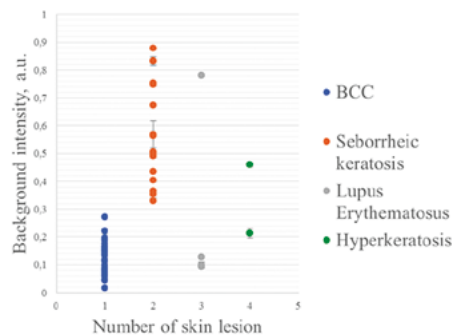


Fig. 1. Scatter plot of the background intensity A parameter for all basal cell carcinomas (1), seborrheic keratoses (2), lupus erythematosus and hyperkeratoses (4).

To summarize the proposed technique and data processing method seems to be a good potential for non-invasive differentiation of BCC from seborrheic keratosis and can be implemented as a fast screening method of skin non-pigmented pathologies.

ACKNOWLEDGEMENT

This work has been supported by European Regional Development Fund project "Portable Device for Non-contact Early Diagnostics of Skin Cancer" under grant agreement # 1.1.1/16/A/197.

[1] A. Lihachev et al., Autofluorescence imaging of basal cell carcinoma by smartphone RGB camera, J BIOMED OPT, 20, 120502 (2015)

Optical System of a Microscope Module for Multispectral Quantitative Phase Imaging Based on Acousto-optic Filtration of Light

O. Polschikova^{1,2}, A. Machikhin^{1,2}, V. Batshev¹, A. Ramazanov¹, V. Pozhar¹

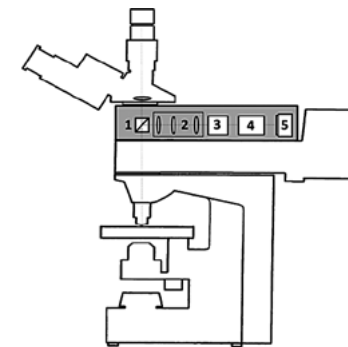
¹Scientific and Technological Center of Unique Instrumentation, Russian Academy of Sciences, Moscow, Russia

²Institute of Automatics and Computer Engineering, National Research University "Moscow Power Engineering Institute", Moscow, Russia

E-mail: polschikova@gmail.com

Quantitative phase imaging is an effective tool for studying weakly absorbing and scattering objects, and can be widely applied in both biomedicine [1] and industry [2]. The aim of the quantitative phase imaging methods is to obtain a two-dimensional map of light wave phase delay introduced by the object. Recent research in this area has shown that use of wide-band light sources in many cases is more effective than laser sources, since low-coherent light provides better phase retrieval sensitivity due to reduced speckle and noise. Another advantage of white light is that it may be used for multispectral imaging techniques.

In this study, we propose an optical scheme of a compact add-on microscope module for multispectral quantitative phase imaging. The system utilizes acousto-optical tunable filter (AOTF) for high-resolution spectral selection within the wide range of a microscope light source (halogen lamp). The module (see figure) consists of a beamsplitter (1), an optical coupling system (2), the AOTF (3), a common-path interferometer (4) and a digital camera (5). We discuss the main issues concerning conjugation of the module with optical microscopes, particularly the selection of the optimal parameters of the optical coupling system [3] between the microscope and the AOTF.



Multispectral quantitative phase imaging module in conjugation with a microscope:

1 – beamsplitter, 2 – optical coupling system, 3 – acousto-optical tunable filter, 4 – common-path interferometer, 5 – digital camera.

[1] M. Mir et al., Quantitative Phase Imaging, Progress in Optics, Vol. 57, 133-217 (2012).

[2] D. Dotti et al., Quantitative phase imaging applied to laser damage detection and analysis, Appl. Opt., Vol. 54, 8375-8382 (2015).

[3] A. Machikhin et. al., Double-AOTF-based aberration-free spectral imaging endoscopic system for biomedical applications, Journal of Innovative Optical Health Sciences, Vol. 8, No. 3, 1541009 (2015).

First Results of Cavity Ring down Signals from Exhaled Air

G. Revalde^{1,2}, K. Grundšteins^{2,3}, J. Alnis³, A. Skudra³

¹Department of Material Science and Applied Chemistry, Institute of Technical Physics, Riga Technical University, Riga, Latvia

²Smart Technology Centre, Ventspils University College, Ventspils, Latvia

³Institute of Atomic Physics and Spectrometry, University of Latvia, Riga, Latvia

E-mail: gitar@latnet.lv

Human breath analysis is known as a non-invasive diagnostic method to detect different diseases. Human breath contains many volatile organic compounds (VOC) in very low concentration. Our goal is to create system for diagnostics of the early stage lung cancer by detecting biomarkers of the disease in the exhaled air. We have built a cavity ring-down system (CRDS) that would allow detecting low intensity VOC signals. Cavity ring down spectrometry is a very sensitive spectrometric technique that avoids typical absorption sensitivity limitations. This method allows detecting low signals in a real time without preconcentration. Our CRDS is a portable system that works in UV region with the pulsed Nd:Yag laser at 266 nm [1]. The core part of the CRDS system is a resonator with high reflectivity mirrors at the both ends. A PMT and an oscilloscope register the CRDS signals. The breath samples are collected in the bags. The bags are attached to the CRDS system and the air is pumped into resonator. The concentrations of biomarkers are calculated from the exponential fit to the ring-down signal. In our experiment, first results from breath samples from volunteers after doing different activities were collected and examined. Influence of the smoking on the breath signals also was examined. An example of the signal of exhaled air before and after physical activity is shown in Fig. 1.

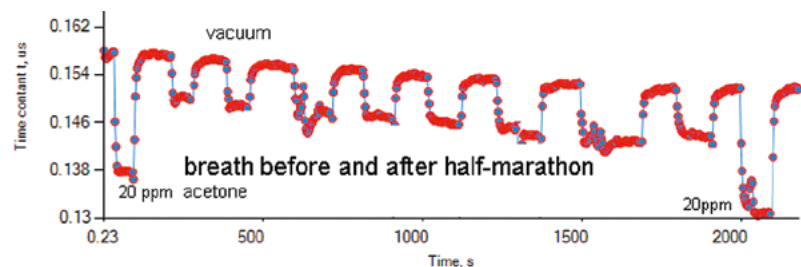


Fig. 1. An example of the CRDS breath signal from the volunteer: before and after half – marathon.

ACKNOWLEDGEMENTS

G.Revalde and K.Grundšteins acknowledge the partial support from the National Research Programme "The next generation of information and communication technologies" (NexIT).

Estimation of the Effect of Radionuclide Contamination on Vicia Sativa L. Induction of Chlorophyll Fluorescence Parameters Using "Floratest" Optical Biosensor

Yu. Ruban, V. Illienko, N. Nesterova, O. Pareniuk, K. Shavanova

National University of Life and Environmental Sciences of Ukraine, Kyiv, Ukraine

E-mail: yuliya_ruban@mail.ua

Nowadays approximately 20% of arable land in Ukraine is contaminated by ¹³⁷Cs and ⁹⁰Sr due to the Chernobyl disaster. This fact affects severely crops development, including its photosynthetic apparatus. To determine the effect of radionuclides on plants growth, it is advisable to use express and effective instruments, which can be used both in the laboratory and in the field. Therefore "Floratest" biosensor system, based on the induction of chlorophyll fluorescence (IChF), is widely used in modern studies of photosynthetic processes. It allows implementing permanent and safe control of the physiological condition of plant development and photosynthetic process, which significantly increases the effectiveness of plant growing intensive.

The presented research was aimed to determine the parameters of IChF curve for *Vicia sativa* L. that were grown on radionuclide contaminated soils with assessment using "Floratest" fluorometer. Plants were inoculated with 5 species of bacteria that might potentially block radionuclide uptake (*Agrobacterium radiobacter* IMBB-7246, *Azotobacter chroococcum* UKMB-6082, *A. chroococcum* UKMB-6003, *Bacillus megaterium* UKMB-5724, *Rhizobium leguminosarum* bv. *viciae*) and grown in sod-podzolic, chernozem and peat-bog soils, contaminated with ¹³⁷Cs (4000±340 Bq/kg).

Morphometric and IChF curve parameters for vetch plants were measured after 14 days of cultivation. On poor sod-podzolic soil most effective inoculants were *A. chroococcum* UKMB-6003 and *A. radiobacter* IMBB-7246. *A. chroococcum* UKMB-6082 and *R. leguminosarum* inhibited plant growth. Regarding peat bog soils, improved morphometric parameters of plants that were inoculated with *A. chroococcum* UKMB-6003, *B. megaterium* and *R. leguminosarum*. For chernozem soils, best effect was shown by *R. leguminosarum* and UKMB-6082. *A. chroococcum* UKMB-6003 and *A. radiobacter* IMBB-7246 show little effect on plant growth and development.

As to compare the effects of different strains of microorganisms inoculation, it should be noted that variants with inoculation of all strains of microorganisms in experiments with vetch statistically differed from controls. Thus the variant with seed inoculation vetch *R. leguminosarum* was observed for the highest level of the culture of accumulation ¹³⁷Cs. The remaining strains conversely reduced transition of radionuclides from the soil.

IChF curves for plants vetch that were grown on typical chernozem with microorganisms shows that the most stressful factor that worsened the performance of the photosynthetic apparatus of plants was inoculation *A. chroococcum* UKMB-6082, while the most positive was inoculation by *R. leguminosarum*. In peat-bog soils worst impact on the plant showed almost all types of bacteria that were used during the experiment except *A. radiobacter* IMBB-7246. Compared with the control inhibit effect were in vetch plants that inoculated with *B. megaterium* UKMB-5724. In sod-podzolic soil improving properties show bacteria *A. chroococcum* UKMB-6082, *A. chroococcum* UKMB-6003 and *R. leguminosarum*.

Thus, the results of the studies showed that the biggest stress factor for plants in terms of radioactive contamination of the soil was inoculation strain of *B. megaterium* UKMB-5724 in each type of analyzed soil, demonstrating as an increase in the number of inactive chlorophyll. Other bacteria showed radioprotective properties in nearly all soils. Summing up the data, we can conclude that when growing plants in the contaminated areas must take into account the type of soil and select different types of bacteria according to them.

[1] G. Revalde et al, Cavity Ring-Down Spectroscopy measurements of Acetone concentration, IOP Conf. Series: Journal of Physics: Conf. Series 810 (2017) 012036.

The Immune Biosensor for Ochratoxin-A Detection Based on the Surface Plasmon Resonance Effect

N. Shpyrka, Y. Ruban, O. Pareniuk, K. Shavanova

National University of Life and Environmental Sciences of Ukraine, Kyiv, Ukraine

E-mail: Nelya_Slyshyk@mail.ru

Ochratoxin-A (OTA) is one of the most dangerous mycotoxins. It is a natural contaminant of grains and legumes, produced by *Aspergillus* and *Penicillium* fungi [1]. Therefore, it is important to control the in real time quality parameters and the presence of mycotoxins in products at all stages of cultivation, processing and transportation of products [2, 3]. The model study is aimed for detecting Ochratoxin-A by surface plasmon resonance-based (SPR-4M) optical biosensors (Glushkov Institute of Cybernetics (GIC) of National Academy of Sciences of Ukraine (NASU))

50 nm-thick gold film was prepared by vapour deposition of metal on the glass surface of a prism. To achieve high density of the immune components immobilization on the transducer surfaces, it was preliminarily treated by polyelectrolytes (polyallylamine hydrochloride (PPA)) followed by treating by protein A from *Staphylococcus aureus* 15 min (20 mg/ml) to achieve oriented immobilization of specific antibodies in advance. After that, material was incubated for 15 min in 20 µg/mL of OTA Ag containing solution. To prevent nonspecific adsorption, additionally samples were incubated with bovine albumin serum (BSA). The washing of the device cell was done after each stage of the experiments. The rate of reagent sedimentation on the transducer surface was monitored by the change in the angle of reflection on the device-delivered sensorogram. For each solution the exposure time 15 minutes at a temperature 25°C as further changing the angle of reflection was not observed.

Our results evidence the possibility to detect Ochratoxin-A at the concentration starting from 0.025 ng/ml to 2 ng/ml.

All the mentioned above data shows that SPR-based immune biosensor may be recommended both for screening observation of environmental objects and for verification of preliminary obtained results by any other approaches.

Implicit Dosimetry of Microorganism Photodynamic Inactivation

M. Tamošiūnas, N. Kuliešienė, R. Daugelavičius

Department of Biochemistry, Faculty of Natural Sciences, Vytautas Magnus University, Lithuania

E-mail: m.tamosiunas@gmf.vdu.lt

Our study shows the feasibility of protoporphyrin IX (Pp IX) photobleaching for predicting the efficacy of *C. albicans* and *S. aureus* photodynamic inactivation. For some photosensitizers, photobleaching occurs due to the photosensitizer interaction with singlet oxygen or other radicals which have already been produced by photodynamic reaction. Therefore the efficacy of microorganism killing could be quantified during each individual photodynamic treatment implicitly, by monitoring photobleaching after the application of exact photosensitizer concentration and the exact light dose.

For the experimental proof, *C. albicans* and *S. aureus* cultures were overnight grown on Sabouraud dextrose or Lysogeny broth, correspondingly, with shaking at 30 °C or 37 °C. Cells were pelleted by centrifugation and resuspended in PBS (pH = 7.4) to obtain 1.8×10^7 cfu ml⁻¹ for *C. albicans* or 1.8×10^9 cfu ml⁻¹ for *S. aureus*. The cells were further incubated with 50 µM of Pp IX for 10 min and irradiated by 473 nm light at 45 mW/cm², up to the light dose of 20 J/cm² for *C. albicans* or 10 J/cm² for *S. aureus*. The survival of the microorganisms was assessed by counting the cell colonies formed after 48 h growth for *C. albicans* or, respectively, after 18 h for *S. aureus*.

Surviving fractions of *S. aureus* or *C. albicans* were plotted versus PpIX photobleaching degree (F_t/F_0) under continuous light mode or pulsed light (5 Hz modulation; 100 ms pulses; 50 % duty cycle) irradiation. Data show that the loss of PpIX fluorescence was linearly proportional to the decrease of microorganisms' viability within the examined light dose range. Therefore we demonstrated that higher degree of PpIX fluorescence photobleaching (F_t/F_0) corresponded to improved killing efficacy of both *C. albicans* and *S. aureus* cells.

The spectroscopic data allowed further insights into PpIX-based photodynamic inactivation of *C. albicans* and *S. aureus*. The significant increase in F_t/F_0 same as increase in PpIX photobleaching decay constant τ (from 2.86 ± 0.32 J/cm² to 1.79 ± 0.06 J/cm²) was produced by the pulsed irradiation regime applied to *S. aureus*, however no analogue effects have been observed for *C. albicans*. The occurrence of oxygen depletion environment possibly resulted after PpIX internalisation, regulated by *S. aureus* cell wall anchored IsdH haem receptor, also by ABC type haem transporters (HrtAB) localized in the plasma membrane. Indeed, the fluorescence maxima of PpIX incubated in *S. aureus* suspension was shifted to the longer wavelengths (635 nm) when compared with the Pp IX fluorescence peak localized at 619 nm in case of *C. albicans*, which resembles PpIX spectra in aqueous solution. For the explanation, at physiological pH the carboxyl group of PpIX is deprotonated ($-COO^-$) and therefore the negative charges of mannosylated glycoproteins in *C. albicans* cell wall initially prevent PpIX entry into the cell. Presumably, the lack of selective Pp IX transporters makes the cell wall of *C. albicans* the primary target of photosensitization. A two-exponential decay in PpIX fluorescence, characterised with initial rapid rate of decay ($\tau = 1.18 \pm 0.21$ J/cm²) and followed by a slower rate of decay ($\tau \approx 7.5$ J/cm²), could evidence the relocation of PpIX during photodynamic inactivation, starting after the significant portion of PpIX has been decomposed outside *C. albicans*.

In conclusion, our study reports the potential of Pp IX photobleaching incorporation into the dosimetry of *C. albicans* and *S. aureus* photodynamic inactivation. Photobleaching as the implicit dose metric has not yet been reported for any pathogen treatment.

[1] J. L. Richard, Some major mycotoxins and their mycotoxicoses – an overview, Int. J. Food Microbiol., Vol.119, pp. 3-10, (2007).

[2] I. Rodrigues et al., A three-year survey on the worldwide occurrence of mycotoxins in feed stuffs and feed Toxins (Basel), Vol. 4, pp.663–675,(2012).

[3] W. L. Bryden, "Mycotoxin Contamination of the Feed Supply Chain: Implications for Animal Productivity and Feed Security," Animal Feed Science and Technology, Vol. 173, No. 1, pp. 134-158, (2012)

pEGFP Transfection into Murine Skeletal Muscle by Electrosonoporation

**M. Tamošiūnas¹, D. Jakovels², U. Rubins², J. Baltušnikas³, R. Kadikis⁴,
R. Petrovskas⁵, S. Šatkauskas¹**

¹Vytautas Magnus University, Faculty of Natural Sciences, Lithuania

²University of Latvia, Institute of Atomic Physics and Spectroscopy, Latvia

³Lithuanian Sports University, Institute of Sports Sciences, Kaunas, Lithuania

⁴Institute of Electronics and Computer Science, Latvia

⁵Latvian Biomedical Research and Study Centre, Latvia

E-mail: m.tamosiunas@gmf.vdu.lt

Either electroporation or sonoporation alone has become an attractive new strategy for the gene therapy, in part because of minimal toxicity and an excellent safety when compared to other gene transfection methods such as virus vectors. However, the efficiency of gene transfection using electroporation or sonoporation is not sufficient and it remains the main drawback considering the transfer of these methods into clinics.

Previously we demonstrated that electroporation and sonoporation parameters could be varied to increase enhanced green fluorescent protein (EGFP) expression levels in mice *tibialis cranialis* muscle [1]. Taking into account that both electroporation and sonoporation induce pores in cellular plasma membrane we presumed that used in combination, these methods can increase the efficiency of EGFP coding plasmid delivery. This effect has been only investigated in vitro demonstrating the synergism of GFP transfection by applying electrosonoporation [2]. In this study, we present the long-term electrosonoporation effects *in vivo*, employing fluorescence spectroscopy method for gene transfection efficiency quantification.

Based on our previous data, the most efficient transfection of pEGFP (10 µg) into C57Bl/6 mice *tibialis cranialis* muscle was achieved by electroporation, combining 1HV (amplitude 800 V/cm, length of 100 µs) and 4LV (80 V/cm; 100ms; 1 Hz) pulses. Application of 1HV (or 4LV pulses) alone or sonoporation (2 W/cm²; 20% DC, 5 min) alone resulted in much lower GFP expression levels within the whole 1 year period.

The first strategy for electrosonoporation was to substitute either 4LV pulses or 1HV pulse by sonoporation. The second strategy for electrosonoporation was to apply sonoporation before 1 HV electric pulse. Considering the long-time transfection, our data revealed that these successive applications of electroporation and sonoporation could not increase the transfection levels of EGFP. Moreover, both electrosonoporation protocols resulted in significant decrease of GFP transfection levels in comparison to electroporation with 1HV+4LV results.

As expected before the experiment, when electric pulses and ultrasound application are combined one should achieve the summation or even synergistic effects of the therapy. We found by histological muscle examination that muscle fiber damage (necrosis) has been additively increased by electrosonoporation, compared to electric pulses and ultrasound applied groups. Therefore for the first time, we present the significant effect of irreversible electrosonoporation possibly suppressing the EGFP transfection levels.

Application of Fluorescent and Vibration Spectroscopy for Septic Serum Human Albumin Structure Deformation during Pathology

**A. Zyubin¹, E. Konstantinova^{1,2}, V. Slezhkin^{1,2},
K. Matveeva¹, I. Samusev¹, V. Bryukhanov¹**

¹Immanuel Kant Baltic Federal University, Kaliningrad, Russia

²Kaliningrad State Technical University, Kaliningrad, Russia

E-mail: azubin@mail.ru

Sepsis is a systemic pathology that can lead to complications and death [1]. World-wide, up to 13 million people develop sepsis each year, and as many as 4 million people have died [2].

Fluorescent and vibration spectroscopy acts as a perspective instruments for the biomolecules investigation and it conformational changes study [3, 4]. Understanding the structural changes of the human albumin, at the molecular level, during pathology, is a key for development of new methods of in-vitro diagnostics.

In this paper we perform results of conformational analysis carried out by Raman spectroscopy, IR spectroscopy and fluorescent spectroscopy of septic human serum albumin. RS spectra were registered at Centaur U science unit equipped with 632 He-Ne excitation source. IR spectra were obtained on Shimadzu IR-Prestige-21 in the range of 500-4000 cm⁻¹ with a resolution of 4 cm⁻¹. Fluorescence spectra were obtained by Fluorolog-3 scientific unit. The main vibrational groups were identified and analysed for septic HSA and its health control. Comparison between Raman and IR results were done. Fluorescent spectral changes of Trp 214 group were analysed. Applications of Raman, IR spectroscopy, luminescent spectroscopy for conformational changes study of HSA were shown.

[1] Tamosiunas et al., Noninvasive optical diagnostics of enhanced green fluorescent protein expression in skeletal muscle for comparison of electroporation and sonoporation efficiencies, *Journal of Biomedical Optics*, 21, 45003 (2016).

[2] Escoffre et al., In vitro gene transfer by electrosonoporation, *Ultrasound in Medicine and Biology*, 36, 1746–1755 (2010).

[1] Burgess D. et al., *Anticicrobial regimen selection, Pharmacotherapy a pathophysiologic approach*. 6th ed, pp. 1920–1921 (2005).

[2] Levy M. et al., *ABC of sepsis*, Wiley-Blackwell 2010. p.1 (2010).

[3] Hering et al., SERS: a versatile tool in chemical and biochemical diagnostics, *Analytical and Bioanalytical Chemistry*, vol. 390, pp 113-124 (2008).

[4] Barth A., *Infrared spectroscopy of proteins*, *Biochimica et Biophysica Acta (BBA)-Bioenergetics*, vol. 1767, pp 1073-1101 (2007).

Supporting institutions



SPIE.

SLOB

Starptautiskā Lietišķās Optikas biedrība



**LATVIJAS
UNIVERSITĀTE**
ANNO 1919

UNIVERSITY OF LATVIA